SEMMELWEIS EGYETEM

DOKTORI ISKOLA

Ph.D. értekezések

3209.

BODON GERGELY

Alapkutatások klinikai alkalmazása

című program

Programvezető: Dr. Vásárhelyi Barna, egyetemi tanár

Témavezető Dr. Ruttkay Tamás, egyetemi adjunktus

Advanced Posterior Strategies for Upper Cervical Spine Surgery

PhD thesis

Gergely Bodon, MD

Theoretical and Translational Medicine Division

Semmelweis University

Supervisor: Tamás Ruttkay MD, PhD

Official reviewers: Árpád Viola MD, PhD

József Farkas MD, PhD

Head of the Complex Examination Committee:

Miklós Réthelyi MD, D.Sc

Members of the Complex Examination Committee:

Zsuzsanna Arányi MD, PhD,

Áron Lazáry MD, PhD

Budapest

2026

Table of contents

List of abbreviations:

AAJ – atlantoaxial joint

ACC – accessory atlantoaxial ligament

AL – alar ligament

AOJ – atlantooccipital joint

APLM – arch posterior to the lateral mass

C0 – occipital bone

C1 – atlas vertebra

C1PA – C1 posterior arch

C1LM – C1 lateral mass

C2 – axis vertebra

C2B – C2 body

C2G – C2 ganglion

C2L – C2 lamina

C2NR – C2 nerve root

CL – cruciate ligament of the atlas

CT – computed tomography

EOP – external occipital protuberance

L3 – third lumbar vertebra; the number indicates its position within the lumbar spine

LP – lateral portions of the tectorial membrane

OP – odontoid process

OC – occipital body

T12 – twelfth thoracic vertebra, the number indicates its position in the thoracic spine

TAL – transverse ligament of the atlas

TM – tectorial membrane

V3h – horizontal segment of the vertebral artery's third part

V3v – vertical segment of the vertebral artery's third part

VA – vertebral artery

VB – vertebral body

1. Introduction

Surgical approaches to the upper cervical spine navigate one of the most complex anatomical regions of the spine. This area is home to critical structures such as the brainstem, vertebral artery and upper cranial nerves, with numerous anatomical variations in bony, vascular and soft tissue structures adding to its complexity and increased surgical risks.

This dissertation explores the applied anatomy of the upper cervical spine, focusing on two highly specialized surgical techniques: atlantoaxial fusion and the posterolateral approach to the retro-odontoid region. Atlantoaxial fusion is indicated for atlantoaxial instability caused by various conditions, including congenital anomalies, trauma, tumors, degenerative diseases, infections, or rheumatoid arthritis. The posterolateral approach is utilized in cases involving retro-odontoid pseudotumor, dens osteotomy, odontoidectomy or epidural abscesses.

1.1 Evolution of surgical approaches to the upper cervical spine

Mixter and Osgood performed the first posterior atlantoaxial fusion with a braided silk band more than a century ago in 1910 [1]. Gallie described his posterior wiring method in 1939, and Brooks changed it in 1978 [2, 3]. The failure rates of the latter two methods were rather high as described by Coyne [4] and Melcher [5]. Significantly improved stability was achieved by Magerl and Seeman's 1987 introduction of their trans articular screw fixation technique [6]. Goel described a modified plate and screw method to fuse C1 and C2 in 1994 whereas Harms and Melcher published their approach for C1-C2 fusion utilizing a polyaxial screw and rod construct in 2001 [7, 8].

Significant iatrogenic soft-tissue damage is linked to the standard posterior C1-C2 fusion through subperiosteal muscle dissection and retraction, often from the occiput to the C3-4 level. Significant postoperative pain and compromised muscular function could result from this. Takeshita [9] describe it as the posterior ligamentous tension band is disrupted and biomechanics are changed as a result of the soft tissue damage to the upper cervical spine. In addition to increasing the likelihood of postoperative sagittal plane deformity

and adjacent segment disease, open posterior approaches to the cervical spine may result in 18–60% of patients experiencing prolonged postoperative discomfort, muscular spasms, and dysfunction as reported by O'Toole at al. [10].

The most recent advancement in this approach is the use of polyaxial screws and minimally invasive surgical procedures for C1-C2 fusion using Harms´ technique. Several methods have been reported, including a muscle-dilating strategy employing expandable tubular retractors by Joseffer [11], Holly [12], and Taghva [13] and a muscle-preserving technique using intermuscular planes by Shiraishi [14]. We outline the applied anatomy of a minimally invasive a muscle splitting technique to the upper cervical spine.

Minimizing approach-related morbidity is the aim of minimally invasive surgery. Minimally invasive surgery has been shown to have positive effects by stabilizing ligamentous structures, preserving muscles, reducing retraction, devascularization, and denervation of muscles, reducing intraoperative blood loss, reducing postoperative pain and reducing hospital stays [11, 15-17].

The standard posterior approach to the atlantoaxial junction can be extended to access the epidural space and the retro-odontoid region.
Up until now, several surgical approaches to the retro-odontoid region have become available. Anterior approaches include the transoral, high cervical retropharyngeal, or Whitesides approach. However, when an anterior approach is performed initially, a second-stage surgery is required for posterior instrumentation and fusion.

Posterior surgical access to the retro-odontoid region can be achieved through the posterolateral transcondylar approach and the posterolateral extradural suboccipital approach.

The posterolateral transcondylar approach requires significant removal of bone from the occipital condyle, which often necessitates additional cranio-cervical fusion.
In contrast, the posterolateral extradural suboccipital approach includes a standard posterior midline incision and reaches the retro-odontoid region obliquely, circumventing

the spinal cord. This approach offers several advantages, including theability to perform decompression, instrumentation, and fusion within the same procedure, thereby eliminating the need for staged surgery.

The choice of surgical approach is determined on a case-by-case basis, considering the specific location, extent, and nature of the pathology. This individualized decision-making process ensures that the selected technique provides optimal access while minimizing risks to surrounding structures.

To facilitate safe and effective access to the lateral or ventral epidural and retro-odontoid space, a portion of bone from the posterior arch of the atlas often needs to be removed, allowing surgeons to reach the target area without compromising critical anatomical structures.

Some modifications of the far lateral suboccipital approach have been reported, including the removal of a retro-odontoid pseudotumor [18], to achieve partial odontoidectomy [19], or to drain an atlantoaxial epidural abscess [20]. The authors of these studies describe requiring different degrees of bone resection using their respective approaches.

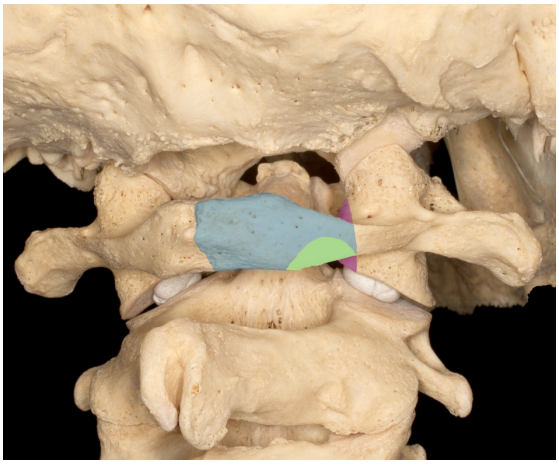

Figure 1. A macerated bone specimen illustrates the three stages of bone removal. Step 1 involves no bone removal, serving as the baseline. Step 2 consists of a semicircular laminotomy, indicated in green. Step 3 involves the resection of the blue-marked posterior hemiarch. Step 4 includes the removal of the purple-marked bone from the medial aspect of the C1 lateral mass. Reprinted with permission; Bodon 2020 [21]

1.2 Surgical anatomy of the upper cervical spine and the craniocervical junction

The most complex area of the spine is most likely the craniocervical junction. It is crucial to understand the anatomy of this area in order to prevent disastrous surgical problems. The occipital bone, atlas, and axis vertebrae make up the craniocervical junction. The form and direction of these three bones' joint surfaces, as well as the guidance provided by their ligaments, dictate their respective movements. The medulla oblongata is situated at the level of the clivus and the foramen magnum, the spinal cord is found in the vertebral canal of the atlas and the axis. The bony architecture, suboccipital muscles and the pertinent ligamentous structures of the craniocervical junction are the main topics of this chapter.

1.2.1 Bony anatomy

The occipital bone's (Figure 2) primary function in surgical procedures is to serve as an anchor during occipito-cervical fusion. The foramen magnum can be oval (42%) or round (58%), according to Cirpan [22]. The occipital bone consists of three distinct parts: the squamous portion, paired condylar portions, and the basal portion. The clivus, located anterior to the foramen magnum, is formed by the basal portion of the occipital bone. It measures 42.8 mm in length from the basion to the sella's midpoint, and it ascends anterocranially at a 45° angle [23].

At the level of the clivus lie the pons and a portion of the medulla oblongata. The occipital condyles are situated within the paired condylar portions, lateral to the foramen magnum. These oval-shaped condyles feature long axes oriented anteriorly and laterally, articular surfaces that face inferiorly and laterally, and a posterior pole that extends to the center of the foramen magnum. The dimensions of the condyles are as follows: they measure 23.26 mm and 20.85 mm in length, 12.54 mm and 11.51 mm in breadth, and 9.63 mm and 9.03 mm in height. The convergence angles of the condyles differ slightly between sexes, measuring 27.34° in males and 29.05° in females [24].

Approximately 9.5mm cranial to the condyle's articular surface the hypoglossal canal opens on the occipital bone [24]. The canal's medial border is located 21.3 mm from the

midline [25]. The alar and the accessory ligaments attach to the rough medial surface of the occipital condyle (Figure 2c) [26, 27].

The condylar fossa, located behind the condyles, is occasionally perforated by an emissary vein (Figure 2a). The squamous part of the occipital bone, which is positioned posterior to the foramen magnum, forms a concave plate. Its outer surface provides attachment sites for muscles and ligaments (Figure 2a). The external occipital protuberance (EOP) is the most prominent and significant bony landmark marking the midline.

The ligamentum nuchae attaches to a crest that extends caudally from the EOP along the midline to the foramen magnum. The superior nuchal line, which extends laterally from the EOP, serves as an attachment site for several muscles: the sternocleidomastoid and splenius capitis muscles attach to its lateral half, while the trapezius muscle attaches along the midline.

The inferior nuchal line is positioned approximately midway between the external occipital protuberance (EOP) and the foramen magnum. The superior obliquus capitis muscle attaches laterally, while the semispinalis capitis muscle attaches medially, occupying the space between the superior and inferior nuchal lines. Below the inferior nuchal line, the rectus capitis posterior major muscle attaches laterally, whereas the rectus capitis posterior minor muscle attaches medially, spanning the area between the foramen magnum and the inferior nuchal line.

Individual variations in occipital bone thickness can be rather significant. The thickest bone stock is observed at the level of the EOP, measuring an average of 17.5 mm in men and 15.3 mm in women. There is a possibility for screw placement up to 8mm in length in the region extending approximately 2 cm laterally from the EOP at the level of the superior nuchal line and about 3 cm inferior to its center [28].

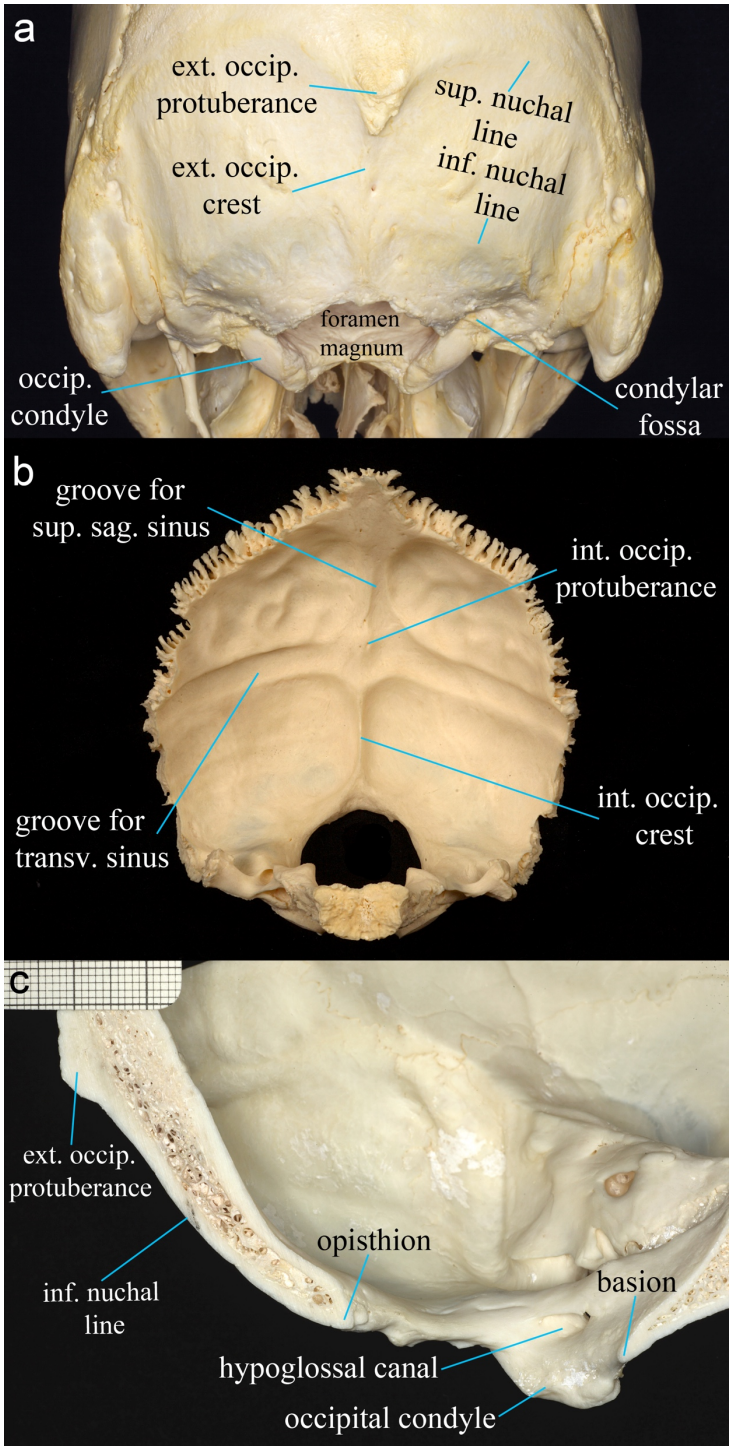

Figure 2. Anatomical features of the occipital bone and surrounding structures. Reprinted with permission; Bodon 2019 [29]

The ring-shaped atlas vertebra (C1) consists of two lateral masses connected by an anterior arch and a posterior arch (Figure 3). The transverse processes extend laterally from the outer sides of the lateral masses.

The anterior longitudinal ligament and the longus colli muscles attach to the anterior arch via the anterior tubercle, which serves as a critical landmark for both radiography and surgery. On the posterior side of the anterior arch, there is a facet joint that articulates with the odontoid process.

The posterior arch exhibits greater variability compared to the anterior arch, forming a continuous bony structure with the posterior roots of the transverse processes. The segments that form this arch vary in both thickness and shape. The midpoint of the posterior arch is marked by a posterior tubercle, which may present as single, double, irregular (creating a groove), or, in some cases, may be absent altogether [30]. This tubercle serves as an attachment site for the nuchal ligament and the rectus capitis posterior minor muscle.

The vertebral artery grooves on either side of the posterior arch, along with the indentation where the vertebral artery crosses the superior aspect of the arch, laterally define the thick middle portion of the posterior arch. The intersection of the outer cortex of the posterior arch and the vertebral artery occurs approximately 20 mm from the midline [31].

The thinnest section of the posterior arch is located lateral to and beneath the vertebral artery groove. This portion of the arch lies posterior to the lateral mass, considering the medial angulation of the lateral mass; hence, it has been termed the arch posterior to the lateral mass (APLM) [32]. This region is particularly important because it serves as the optimal entry site for a posterior arch lateral mass screw [32], whereas the entry point for a lateral mass screw is positioned inferiorly. The posterior root of the transverse process is increasing in thickness compared forming the arch lateral to the APLM.

When the posterior atlanto-occipital membrane becomes partially or fully ossified, it forms a foramen encircling the vertebral artery, referred to as a complete or incomplete ponticulus posticus. In some patients, an oval-shaped supplementary opening, either open or closed, is present posterior to the transverse foramen of the atlas. In other cases, this feature appears only as an indentation. This retrotransverse foramen or groove houses the

anastomotic vein, which connects the venous sinuses above (the suboccipital cavernous sinus) with the vertebral artery venous plexus located below the posterior arch of the atlas [33, 34].

The anterior and posterior arches of the atlas connect the oval bony cylinder that forms the lateral mass, which is covered by joint surfaces on both its superior and inferior sides. The long axis of the lateral mass converges anteriorly at an angle of approximately 18.6° (range: 15.5°–21.8°) [35]. The superior articular surface of the lateral mass is irregular in shape, bean-shaped, and concave, facing medially to support the occipital condyle. In contrast, the inferior articular surface is smaller, rounded, and slightly concave. Due to the tilt of the joints, the lateral mass measures 12.9 mm in height laterally (range: 8.7–17.3 mm) but it narrows to 4.1 mm medially (range: 1.4–6.7 mm). The medial wall of the lateral mass is located 10.2 mm from the midline (range: 8.9–12.8 mm) [35].

The length of the lateral mass, just below the APLM is 17.55mm (measured perpendicular to its long axis) while its width is 17.15 mm [36]. A lateral mass screw can be placed on the posterior surface of the lateral mass, inferior to the APLM, within a working area measuring 4.4 mm in height and 8.4 mm in width [37].

Several studies have reported findings on the height of the groove, C1 posterior arch, pedicle analog, and posterior-lateral arch. These studies indicate that the proportion of arches measuring less than 4 mm in height is 8% (Tan, 2003), 12% (Ma, 2009), 53.8% (Lee, 2006), and 19.2% (Christensen, 2007) respectively [38-41]. In our analysis, we found that the height of the APLM was less than 4 mm in 40.5% of cases [32].

The inner ring of the atlas vertebra's cortical bone, measuring up to 3.5 mm in thickness, is located where the lateral mass meets the posterior arch. On the medial surface of each lateral mass, there is a small bump that serves as the attachment site for the transverse atlantal ligament. In some cases, a bony crest extends along the medial edge of the lateral mass, running posteriorly from just below this tubercle—slightly cranial to the inferior joint surface—to the posteromedial margin of the superior joint surface.

This crest serves as the attachment site for the accessory atlantoaxial ligaments. At the level of the atlas, the spinal canal is relatively large, with the posterior two-thirds forming the canal itself and the anterior third occupied by the dens axis. On MRI measurements, the distance from the tectorial membrane to the anterior aspect of the posterior arch of the atlas ranges from 10.7 to 19.7 mm, with this measurement being proportional to body height and larger in men than in women. The spinal cord, measuring between 7.9 and 8.5 mm at the level of C1, was found to be inversely related to a person's height [42].

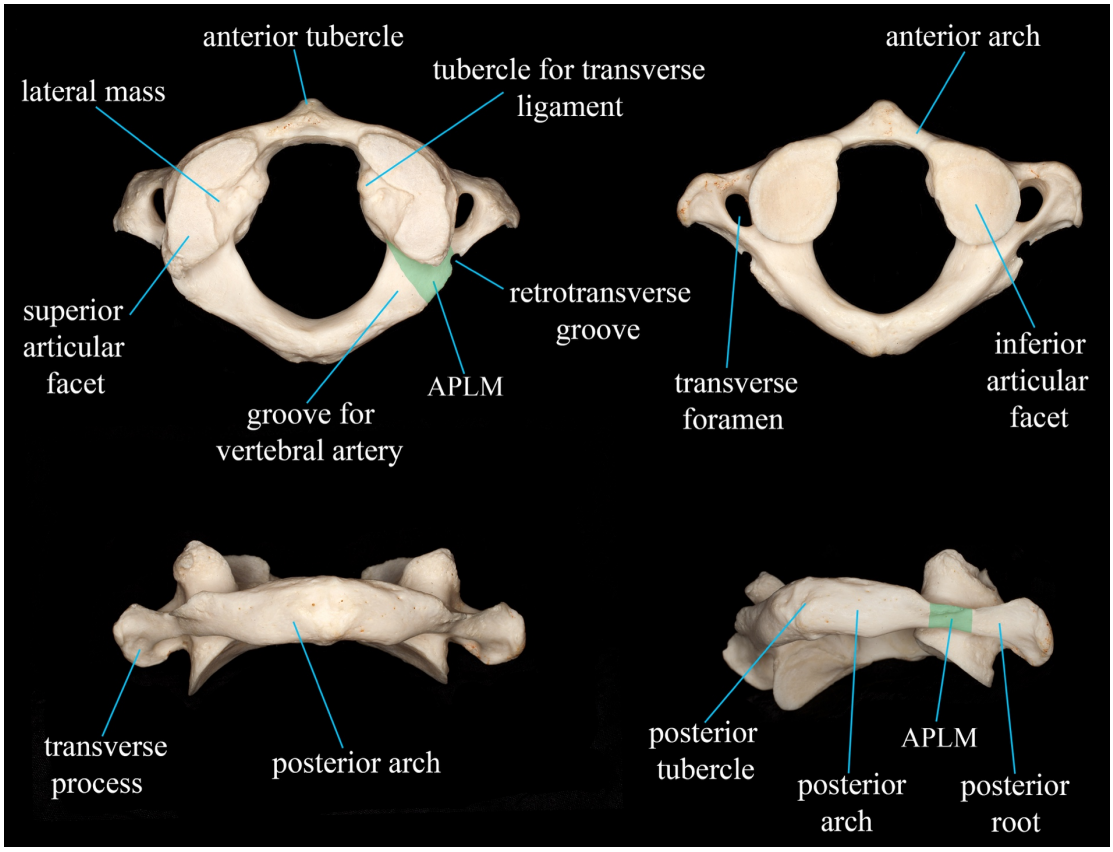

Figure 3. Anatomical features of the atlas (C1) vertebra. Top left: superior view; top right: inferior view; bottom left: posterior view; bottom right: lateral view. APLM – arch posterior to the lateral mass. Reprinted with permission; Bodon 2019 [29]

The axis, or second cervical vertebra, is structurally unique (Figure 4). Its odontoid process (dens) extends cranially from the vertebral body, serving as a pivot around which the atlas, supporting the skull, rotates. The asymmetrical vertebral body features a prominent anteroinferior lip and a concave endplate. The base of the vertebral body is the widest part, with a coronal width of 15.9 mm (range: 12.2–20.1 mm) and a sagittal width

of 16.7 mm (range: 13.6–20.0 mm) [35]. The vertebral body has a height of 22.13 mm (range: 17–26 mm) up to the base of the dens. The dens itself has a mean maximal width of 10.8 mm in the coronal plane and 10.9 mm in the sagittal plane [35], with a height of 15.8 mm (range: 9–21 mm) [43]. Structurally, the dens is composed of thick cortical bone and contains a thin inner spongiosa measuring 4.3–6.2 mm [44].

The dens have a posterior incline at an angle ranging from 0° to 30° relative to the axis body [43]. On its anterior surface, the dens have a joint for articulation with the atlas, while its posterior surface features a transverse groove for the attachment of the transverse atlantal ligament. The oval superior articular facets are located on the upper surface of the two lateral masses, positioned laterally to the vertebral body. To support the lateral masses, two lateral bony pillars extend craniolaterally from the sides of the axis body in the coronal plane. The term "C2 pedicle" is often ambiguously used in the literature, as the genuine anatomical pedicle differs significantly from the surgical pedicle. Additionally, the pars interarticularis region of C2 is frequently and mistakenly referred to as the surgical pedicle. The pars interarticularis is well defined in the lumbar spine as the bony region connecting the superior and inferior joints while the pedicle is the bony structure connecting the vertebral body with the posterior elements. The same analogy can be applied to the cervical spine and to the axis vertebra.

The real anatomical pedicle of the axis is a bone stock that connects the base of the dens to the lateral mass and exits the vertebral body in the coronal plane (Figure 4, middle image) [45, 46]. In contrast, the surgical pedicle is the hemitubular structure that connects the inferior articular process to the vertebral body. It is located medial to the transverse foramen, medial to the vertebral artery groove, and beneath the posteromedial portion of the superior articular process [47]. Specifically, it is the bone stock extending from the lateral bony pillar of the vertebral body to the anteriormost portion of the inferior articular process (Figure 4, lower left image). The surgical pedicle defines the cranial boundary of the inferior vertebral notch of C2, while the pars interarticularis links the superior and inferior articular processes (Figure 4, lower right image). The medial walls of the pars interarticularis and the surgical pedicle share a common origin anterior to the inferior articular process. Together, these structures form the medial wall of the spinal canal.

The vertebral artery enters the vertebral artery groove of the axis, a bony canal, where it travels cranially before turning laterally and exiting through the transverse foramen. The vertebral artery remains in close contact with the bony structures of the vertebral artery groove. The surgical pedicle forms the posteromedial boundary of the groove, while the lateral bony pillar of the vertebral body forms its medial border. The lateral mass constitutes the anterosuperior border, and the pars interarticularis forms the posterosuperior border. Any increase in this groove's dimensions in any direction will reduce the bone stock of the surrounding structures, thereby decreasing the available bone stock for screw placement.

If there is a "high riding" arch present that extends either cranially or posteriorly, it results in a narrowing of the pars interarticularis [48], while a medial extension results in the size reduction of both the surgical pedicle and the lateral bony pillar. In cases of a high-riding vertebral artery, there is often a combination of medial and cranial expansions in the groove's dimensions.

The thickness of the screw in the horizontal plane is the primary limiting factor for screw placement into the axis's pedicle. Measurements using CT angiographies revealed that the mean distance between the medial border of the pedicle and the medial border of the groove is 6.38 mm (range: 2.09–12.62 mm) [49], while another study using CT scans reported a mean of 5.18 mm (range: 2.2–9.2 mm) [50]. The pedicle height averages 9.7 mm in males and 8.7 mm in females [50], and the average transverse angle of the pedicle is 43.9° [51].

In both the coronal and sagittal planes, the superior articular joints slope inferiorly, while the inferior joints are oriented slightly anterolaterally and face inferiorly. There are small lateral projections called transverse processes originating from the lateral surface of the pars interarticularis, just anterior to the inferior articular facet, and on the anterolateral aspect of the lateral mass. The scalenus medius and splenius cervicis muscles attach inferiorly to its tip, while the intertransversarius muscle attaches superiorly. The lamina of the axis is more prominent and thicker compared to other cervical laminas, with its

inferior half measuring an average thickness of 5.77 mm (range: 1.35–9.77 mm) [52]. The bifid spinous process of the axis is also prominent, particularly on its craniolateral aspect, which serves as an attachment site for the rectus capitis posterior major and obliquus capitis inferior muscles superiorly, and for the nuchal ligament, multifidus, and semispinalis cervicis muscles on its inferior aspect.

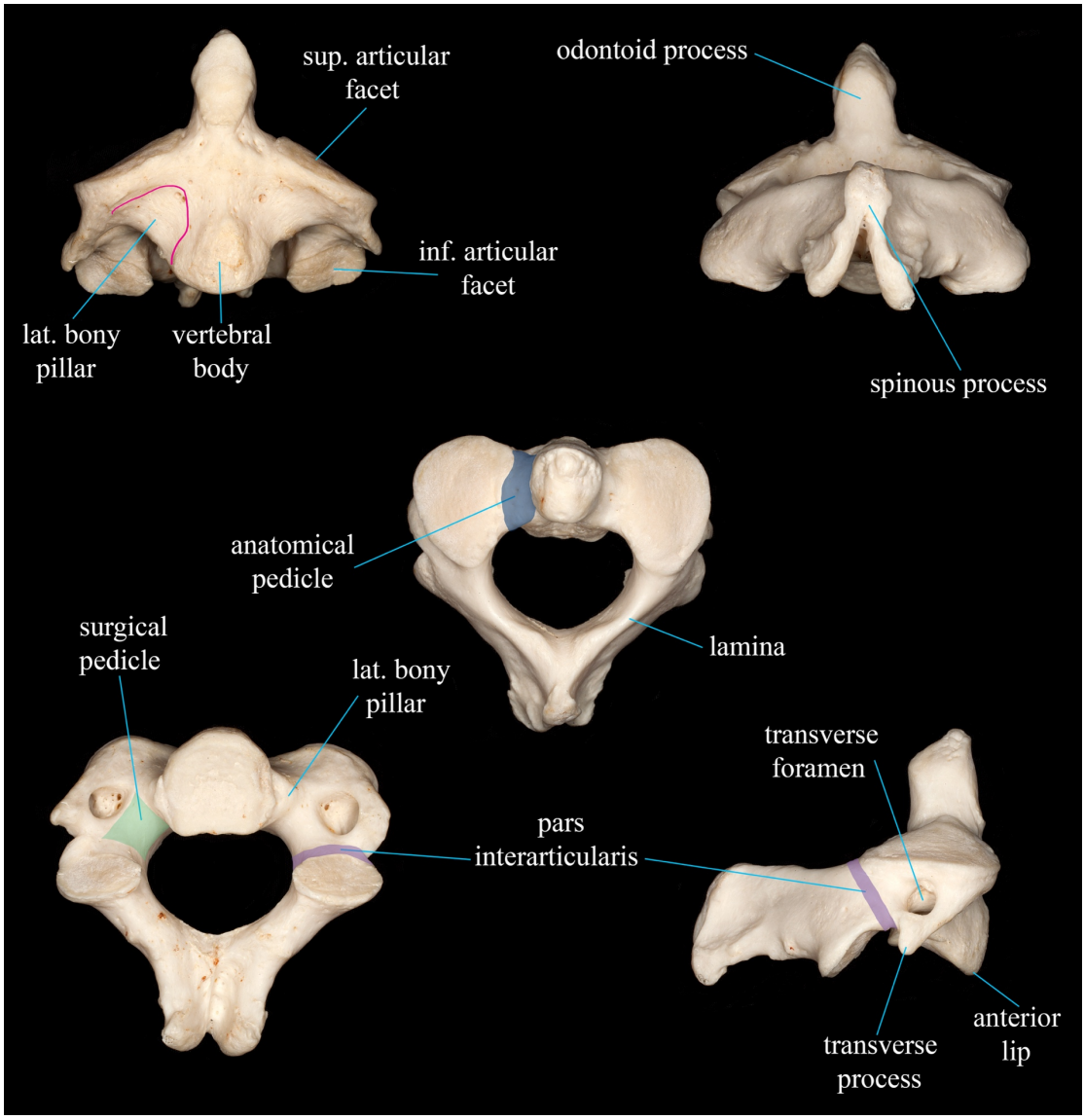

Figure 4. Anatomical features of the axis (C2) vertebra. Top left: oblique posterior view; top right: posterior view; center: superior view; bottom left: inferior view; bottom right: lateral view. Reprinted with permission; Bodon 2019 [29]

1.2.2 Joints, ligaments and membranous structures (Figure 5)

The movement of these bones is dictated by the shape and orientation of their joints, as well as the support of their ligaments. The concave, bean-shaped superior facet of the atlas articulates with the convex occipital condyle, which projects anteriorly and medially, enabling limited lateral flexion and flexion-extension. The oval, slightly convex inferior facet of the atlas faces medially and articulates with the inferiorly sloping, convex superior facet of the axis.

During rotation, the atlas pivots around the dens, which is secured within a ring formed by the transverse ligament and the anterior arch of the atlas. These joints facilitate sliding motions over varying distances depending on the range of movement.

The superior articular processes of the axis bear the weight of the head, transmitted through the lateral masses of the atlas. At the C2-C3 level, this two-column load transitions into a three-column load, where the weight is distributed between the axis's endplate and its two inferior articular processes. This three-column load-sharing system—involving the intervertebral disc with the endplate and the two facet joints—is a structural pattern commonly observed throughout the lower levels of the spine.

The craniocervical junction is stabilized by several key ligaments, including the cruciform ligament—comprising the transverse atlantal ligament and its vertical portion—as well as the paired alar and accessory ligaments and the apical ligament. The tectorial membrane covers these ligaments from the back (Figure 4).

The cruciform ligament (Figure 5b) consists of both horizontal and vertical components, forming a cross-like structure behind the odontoid process. The horizontal segment is primarily made up of the transverse atlantal ligament, which is reinforced by the weaker, vertically oriented longitudinal fibers (Figure 5b). The superior longitudinal fibers extend cranially to the anterior margin of the foramen magnum at the midline, where they fuse with the tectorial membrane, while the inferior fibers attach to the posterior surface of the axis body.

The small tubercle located on the medial surface of the atlas's lateral masses on both sides serves as the attachment point for the transverse atlantal ligament (Figure 5c and 5d). Initially spherical, the ligament flattens and broadens as it extends to envelop the posterior surface of the odontoid process, securing it within the ring formed by the ligament and the anterior arch of the atlas. The ligament measures approximately 18 mm in length, 2 mm in thickness and 10 mm in width at its midpoint [53].

The posterolateral surfaces of the upper third of the dens serve as the origin of the strong, rounded alar ligaments (Figure 5b-d). These ligaments run horizontally and slightly cranially, inserting onto the rough medial surfaces of the occipital condyles. The average diameter of the alar ligaments is 7.3 mm, and their mean length is 8.8 mm [54]. They are partially covered posteriorly by the transverse atlantal ligament, with which they share a close anatomical relationship.

The posteriormost fibers of the alar ligaments form the transverse occipital ligament, which connects the two occipital condyles without contacting the odontoid process. This ligament can be considered a distinct anatomical structure and is reported to be present in 8.3% to 77.8% of cases, depending on the study [55].

The accessory atlantoaxial ligaments (Figure 5b-d), also known as the ligamentum collaterale atlanto-axiale mediale [56], were described by Arnold in 1851 (Arnold’s ligaments) as medial reinforcements of the C1-C2 joint capsules [57].

In the sample we worked on, the accessory ligaments were Y-shaped, the base of the Y originating between the superior articular surface and the base of the dens on the posterior part of the C2 vertebral body. In some specimens, a tubercle was observed at this site. The lateral arm of the Y extended posteriorly from the tubercle of the transverse ligament, attaching to the medial aspect of the atlas lateral mass along a line that ascended toward the posteromedial edge of the superior articular facet.

In some cases, a bony crest along this line marks the attachment site of the supplementary ligaments. The medial arm of the Y, representing the cranial extension of the auxiliary

ligament, merged with the lateral portion of the alar ligament and attached to the medial surface of the occipital condyle, slightly above and posterior to the attachment point of the alar ligament (Figure 5d).

The accessory ligaments, in conjunction with the alar ligaments, likely play a key role in restricting rotation and flexion at the C1-C2 joint. In a cadaver study, Tubbs examined this ligament and referred to it as the accessory atlantal-axial-occipital ligament, reporting its dimensions as 29 mm in length and 5.5 mm in width [27]. On MRI, the C1-C2 segment of the ligament measured 2.8 × 1.8 mm on average, while the thinner C0-C1 segment measured 1.6 × 1.2 mm on the right side and 1.8 × 1.4 mm on the left [58].

The apical ligament, located just anterior to the superior portion of the cruciform ligament, spans the supraodontoid gap, extending from the tip of the dens to the anterior margin of the foramen magnum. It has no significant biomechanical function, and recent findings indicate the absence of notochordal tissue in adults [59]. This ligament was identified in 80% of cadavers studied and measures 10–12 mm in length and 2–5 mm in width [26, 55, 56].

The tectorial membrane (Figure 5a), a broad, flat, square-shaped ligament, covers the entire craniocervical junction and upper cervical spine from behind. Wider at its cranial end, it originates on the clivus, between the hypoglossal canals, and extends caudally to the third cervical vertebral body and the posterior surface of the axis, where it transitions into the posterior longitudinal ligament. The tectorial membrane can be divided into two lateral bands and a central medial band. The medial band runs vertically from the posterior surface of the axis to the anterior margin of the foramen magnum, where it merges with the cranial dura. Approximately 1 cm wide, it covers the posterior surface of the dens. The lateral bands originate at the lateral walls of the spinal canal at the level of C2 (near the medial walls of the pars interarticularis) and diverge as they ascend cranially. These lateral portions of the tectorial membrane house the auxiliary atlantoaxial ligaments.

The anterior atlantooccipital membrane connects the anterior arch of the atlas to the anterior rim of the foramen magnum, while the posterior atlantooccipital membrane is a

broad, thin ligament that links the posterior arch of the atlas to the posterior rim of the foramen magnum. Anteriorly, the dura mater attaches to the posterior atlantooccipital membrane, and posteriorly, it is connected to the rectus capitis posterior minor muscle [55]. The first segment of the ligamentum flavum bridges the lamina of the axis and the posterior arch of the atlas.

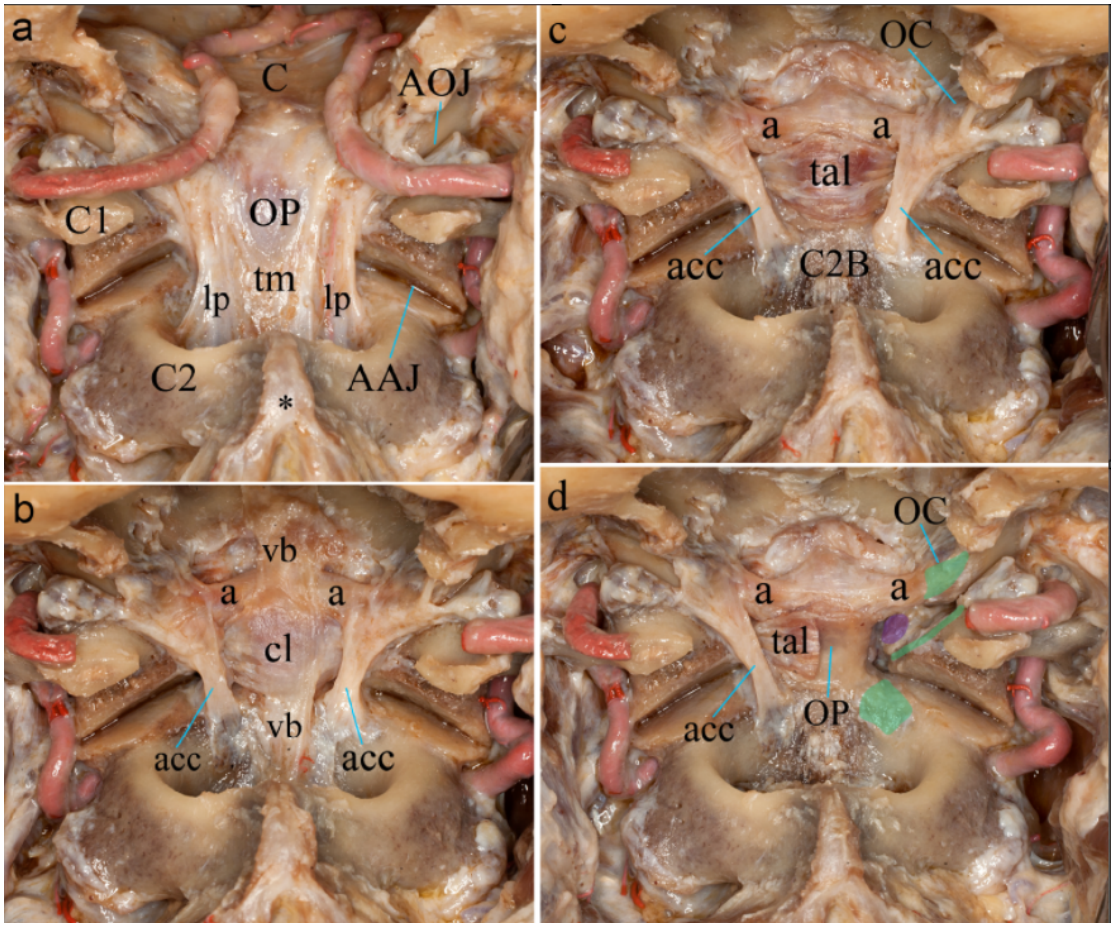

*Figure 5. Ligaments of the craniocervical junction and upper cervical spine. AOJ - Atlanto-occipital joint; AAJ - Atlantoaxial joint; C - Clivus; C1 - Atlas; C2 - Axis; OP - Odontoid process (dens); tm - Tectorial membrane; lp - Lateral portions of the tectorial membrane; * - Base of the odontoid process (dens); cl - Cruciate ligament of the atlas; a - Alar ligament; tal - Transverse atlantal ligament; vb - Vertebral body of C2; acc - Accessory atlantoaxial ligament; OC - Occipital condyle; C2B - C2 body. Reprinted with permission; Bodon 2019 [29]*

1.2.3 Suboccipital Muscles and Nerves (Figure 6)

The fascia covering the suboccipital muscles consists of connective and fatty tissue. The rectus capitis posterior minor originates from the posterior tubercle of the atlas and extends cranially to attach to the occiput, between the foramen magnum and the medial part of the inferior nuchal line.

The suboccipital triangle is an important anatomical region located in the posterior neck, formed by the arrangement of three muscles. These muscles include the rectus capitis posterior major, the obliquus capitis superior and the obliquus capitis inferior. Together, they define the borders of the triangle, which serves as a critical landmark in the suboccipital region.

The rectus capitis posterior major forms the cranial and medial border of the suboccipital triangle. This muscle originates from the spinous process of the axis (C2) and runs cranially and laterally to insert on the lateral portion of the inferior nuchal line of the occiput, just below it. As one of the primary contributors to the triangle, it plays an essential role in defining its medial aspect.

The obliquus capitis superior is responsible for forming the lateral and cranial borders of the triangle. This muscle originates from the upper surface of the transverse process of the atlas (C1) and inserts on the occiput, specifically between the superior and inferior nuchal lines. The insertion point is lateral to the insertion of the rectus capitis posterior major. The obliquus capitis superior travels cranially and dorsally, contributing to the lateral boundary of the triangle.

The obliquus capitis inferior forms the base of the suboccipital triangle. This muscle originates from the spinous process and surrounding lamina of the axis (C2) and extends cranially and laterally to attach to the inferior surface of the transverse process of the atlas (C1). Its positioning at the base of the triangle completes the borders of this key anatomical region.

At the center of the suboccipital triangle lies the vertebral artery groove and the posterior arch of the atlas. The suboccipital nerve, originating from the dorsal ramus of the first cervical nerve (C1), traverses this region. It passes between the posterior groove of the vertebral artery and the horizontal section of the V3 segment of the vertebral artery (V3h – is the segment of the vertebral artery between the transverse process of the atlas and the dural penetration just medial to the atlanto-occipital joint). This nerve is responsible for innervating all three muscles that make up the suboccipital triangle.

Directly beneath the belly of the obliquus capitis inferior muscle lies the C2-C3 joint. Below this muscle, the greater occipital nerve (the medial branch of the dorsal ramus of the C2 nerve) emerges. This nerve travels medially and cranially over the obliquus capitis inferior muscle toward the midline, where it perforates the semispinalis capitis muscle. Lateral to the C2-3 joint, the vertical part of the vertebral artery (V3v) exits the transverse foramen of the axis, turns cranial to enter the transverse process of the atlas. Additionally, the third occipital nerve, which is the sensory superficial medial branch of the third cervical nerve (C3), is located at this region. These nerves play vital roles in sensory innervation of the posterior head and neck.

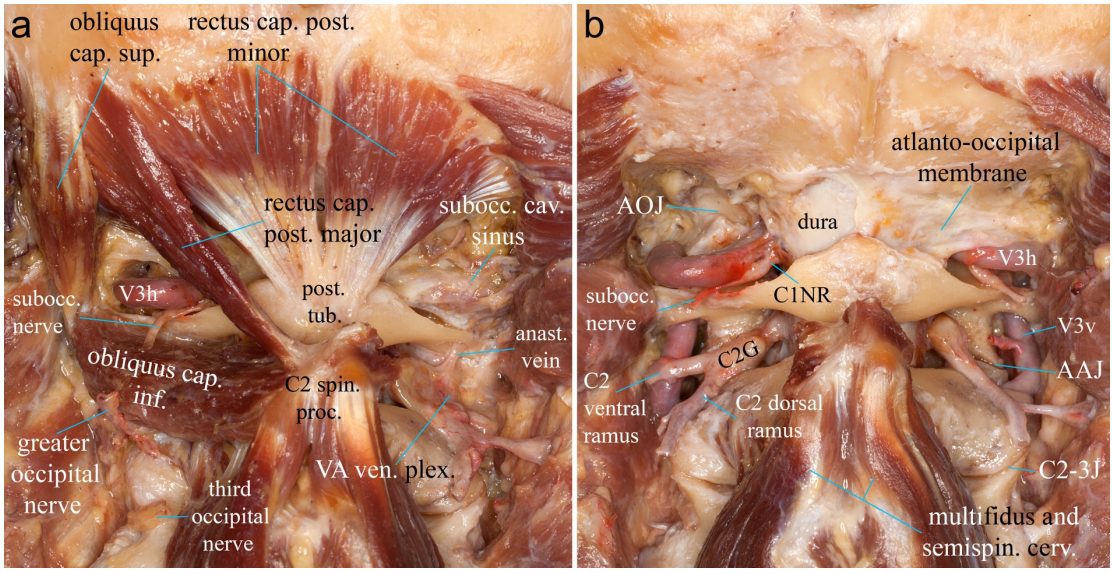

Figure 6. Suboccipital muscles and nerves. Obliquus cap. sup. - Obliquus capitis superior; Obliquus cap. inf. - Obliquus capitis inferior; Rectus cap. post. minor - Rectus capitis posterior minor; Rectus cap. post. major - Rectus capitis posterior major; Post. tub. - Posterior tubercle of C1; C2 spin. proc. - Spinous process of C2; Subocc. nerve - Suboccipital nerve; VA ven. plex. - Vertebral artery venous plexus; Subocc. cav. sinus - Suboccipital cavernous sinus; Anast. vein - Anastomotic vein; C1NR - C1 nerve root; C2G - C2 ganglion; AOJ - Atlanto-occipital joint; AAJ - Atlantoaxial joint; C2-3J - C2–C3 joint; Multifidus and semispin. cerv. - Multifidus and semispinalis cervicis muscles; V3h - Horizontal segment of the vertebral artery; V3v - Vertical segment of the vertebral artery. Reprinted with permission; Bodon 2019 [29]

2. Objectives

The upper cervical spine plays a crucial role in craniovertebral stability and movement. This region is anatomically unique, with complex bony structures, ligamentous attachments and critical neurovascular elements such as the vertebral artery, brainstem, and spinal cord. Due to its biomechanical importance and proximity to vital structures, surgical interventions in this area require high precision and minimal disruption to surrounding tissues.

Traditional posterior approaches to the C1-C2 junction often involve extensive muscle dissection and bone removal leading to increased morbidity, prolonged recovery times and the potential for postoperative complications such as chronic pain and post-surgical instability. As a result, there is growing interest in minimally invasive techniques that aim to preserve musculature while maintaining safe and effective access for instrumentation [60].

To improve surgical strategies for the upper cervical spine, the author of this PhD thesis focused on two key areas, focusing on optimizing minimally invasive and targeted bone removal approaches to improve patient outcomes.

The first article focuses on the applied anatomy and technical feasibility of a minimally invasive, muscle-splitting approach for posterior C1-C2 fusion. The study aimed to determine whether this technique could provide consistent and reliable access to critical anatomical landmarks and screw entry points, specifically for the placement of C1 lateral mass screws and C2 pars interarticularis screws. By thoroughly evaluating the spatial relationships and accessibility of these regions, the research assessed the potential of this approach to minimize muscle disruption while ensuring precise instrumentation [60].

In contrast, the second article examined the amount of bone removal needed to access the retroodontoid region using a posterior far-lateral suboccipital approach. To reach this goal, we measured the size of the surgical window in the horizontal and vertical directions

which were created by stepwise bone resection of the atlas vertebra in three steps in Thiel-fixed human cadavers [21].
Furthermore, both studies emphasized the importance of balancing surgical access with structural preservation. By integrating detailed anatomical analysis with cadaveric feasibility studies, these investigations aimed to refine minimally invasive techniques and optimize instrumentation strategies for the upper cervical spine [21].

Ultimately, this PhD research contributes to the advancement of surgical approaches for C1-C2 fusion and fixation, offering anatomically informed techniques that aim to reduce morbidity, improve surgical precision and enhance patient outcomes.

3. Methods

To describe the relevant anatomy of the upper cervical spine and the craniocervical region macerated dry bone specimens and Thiel fixed cadavers were used [61]. Dry bone specimens of the occipital bone, atlas and axis vertebras were examined to describe and to visualize the bony anatomy. Also, dry bone specimens consisting of the occipital bone, atlas, axis, and the third cervical vertebra were used to visualize the steps of bone removal in the study of the posterolateral extradural suboccipital approach. The bones were held together using UHU Patafix adhesive (Germany). To further investigate the detailed anatomy of the craniocervical junction, three Thiel embalmed cadavers were examined [61].

For the anatomical experimental study on the posterolateral extradural suboccipital approach we used five Thiel-fixed human cadaveric specimens with a mean age of 83.7 years (range 74 to 94). The measurements were performed bilaterally using an electric caliper (Absolute System, Germany). The vertebral arteries were filled with colored (red) silicon before the anatomic dissection. For the dissection, the head was secured in a modified Halo-fixation system (originally used to immobilize the cervical spine in patients with unstable injuries, modified to fix the head during preparation) allowing the cervical spine to remain in a neutral position [60].

The feasibility study of the muscle splitting approach to posterior C1-C2 fusion was started with the examination of the relevant anatomy examined on one formalin fixed and one fresh cadaver. In the latter, the steps of the operation were performed and the relevant soft tissue and bony landmarks visualized. Following this, the approach was performed in 12 fresh human cadavers bilaterally. In four of these cadavers after the muscle splitting approach was performed, the bony landmarks were visualized and the usual 3.5mm polyaxial screws were inserted [21].
Visual aid was used for the anatomical preparations, wherever needed with loupe magnification (Zeiss, 3.4x). During all the studies serving as a basis for this dissertation we performed detailed photo documentation using a Canon 5D digital camera.

The human cadaveric specimens used for the anatomical studies in this thesis were donated to the Department of Anatomy, Histology, and Embryology at Semmelweis University specifically for educational and research purposes. Each donor had signed an official consent document during their lifetime, thereby negating the need for additional approval from an ethics committee for this study.

4. Results

4.1. Muscle splitting approach to posterior C1-C2 approach

As atlantoaxial fusion using a midline posterior approach with a polyaxial screw and rod system is widely practiced, recent efforts have explored minimally invasive variations of this technique. However, the complex applied anatomy of these approaches has not been fully described. Given the unique challenges posed by the C1-C2 complex, particularly due to its bony and vascular anatomy, the author of the present thesis contributed to the conceptualization and execution of a cadaveric study examining the applied anatomy and feasibility of a minimally invasive, muscle-splitting approach for posterior C1-C2 fusion. The author of the present paper has previously published the findings of this study, which also included the results discussed below [60].

In this cadaver-based feasibility study, the first objective was to examine the relevant anatomy of the upper cervical spine. The study hypothesized that the posterior aspect of the atlas and axis vertebrae could be accessed by splitting the muscle layers of the splenius capitis and semispinalis capitis muscles, followed by retracting or resecting the belly of the obliquus capitis inferior. This latter muscle directly overlies the entry points for the atlas lateral mass screws (or posterior arch–lateral mass screws) and the axis pars interarticularis screws. To investigate this, one formalin-fixed cadaver and one fresh cadaver were used. The anatomical dissection was performed under loupe magnification, and a detailed photo-documentation was created [60].

The second objective was to determine whether the anatomical landmarks of the atlas and axis vertebrae could be reliably identified for the placement of atlas lateral mass screws and axis pars interarticularis screws. For this part of the study, the approach was performed bilaterally on 12 fresh cadavers, with 3.5 mm polyaxial screws inserted in four of them. The surgical approach utilized classical dissection techniques, standard retractors and handheld Langenbeck retractors (classic handheld retractor with a 90° bent tip and different lengths) to ensure proper visualization and access [60].

The following section presents a detailed technical description of the C1-C2 muscle-splitting surgical approach, as outlined in the author's previously published work [60]:

The cadaver was positioned prone, and anteroposterior views were taken using a portable C-arm (intraoperatively used X-ray machine used to visualize bony structures and implants) to identify the C1-C2 articulation and articular gap. The C-arm was rotated 10° laterally to one side, and a planned skin incision was marked directly above the entry points for the C1 lateral mass screw and the C2 pars interarticularis screw, extending to the C2-3 joint (approximately 3-4 cm from the midline).

A 3.5 cm-long incision was made to open the skin and nuchal fascia. In some cases, the lateral edge of the trapezius muscle was visible and retracted medially. Beneath the fascia, the fibers of the splenius capitis muscle, running cranially and laterally, were identified, split with scissors, and retracted. Below this, the semispinalis capitis muscle, covered by a thin fascia, was exposed. This muscle, also running cranially, was split and retracted to reveal the underlying structures.

The suboccipital muscles, covered by a layer of fatty fascia, were then exposed. Using blunt dissection, a plane was created between the semispinalis capitis muscle and the suboccipital muscles. The obliquus capitis inferior muscle, running across the surgical field, was identified. Emerging below this muscle was the greater occipital nerve, which was carefully mobilized and protected as it ran along the belly of the obliquus capitis inferior muscle toward the midline.

The obliquus capitis inferior muscle was then prepared, allowing exposure of the posterior arch of the atlas cranially and the C2-3 joint caudally. Depending on the surgical objective (temporary fixation or fusion), this muscle was either retracted or dissected. At this point, the inferior aspect of the posterior arch of the atlas was identified, and the junction of the posterior arch and the midpoint of the lateral mass was exposed using dissectors, working medially to laterally. This allowed identification of the entry point for the C1 lateral mass screw.

Subsequently, the inferior articular process and lamina of C2 were carefully dissected. The superior surface of the C2 pars interarticularis was exposed up to the C1-C2 joint, and its medial border was dissected subperiosteally. This revealed the entry point for the C2 screw. The same procedure was repeated on the contralateral side.

The sequential steps of this technique are illustrated in Figure 7.

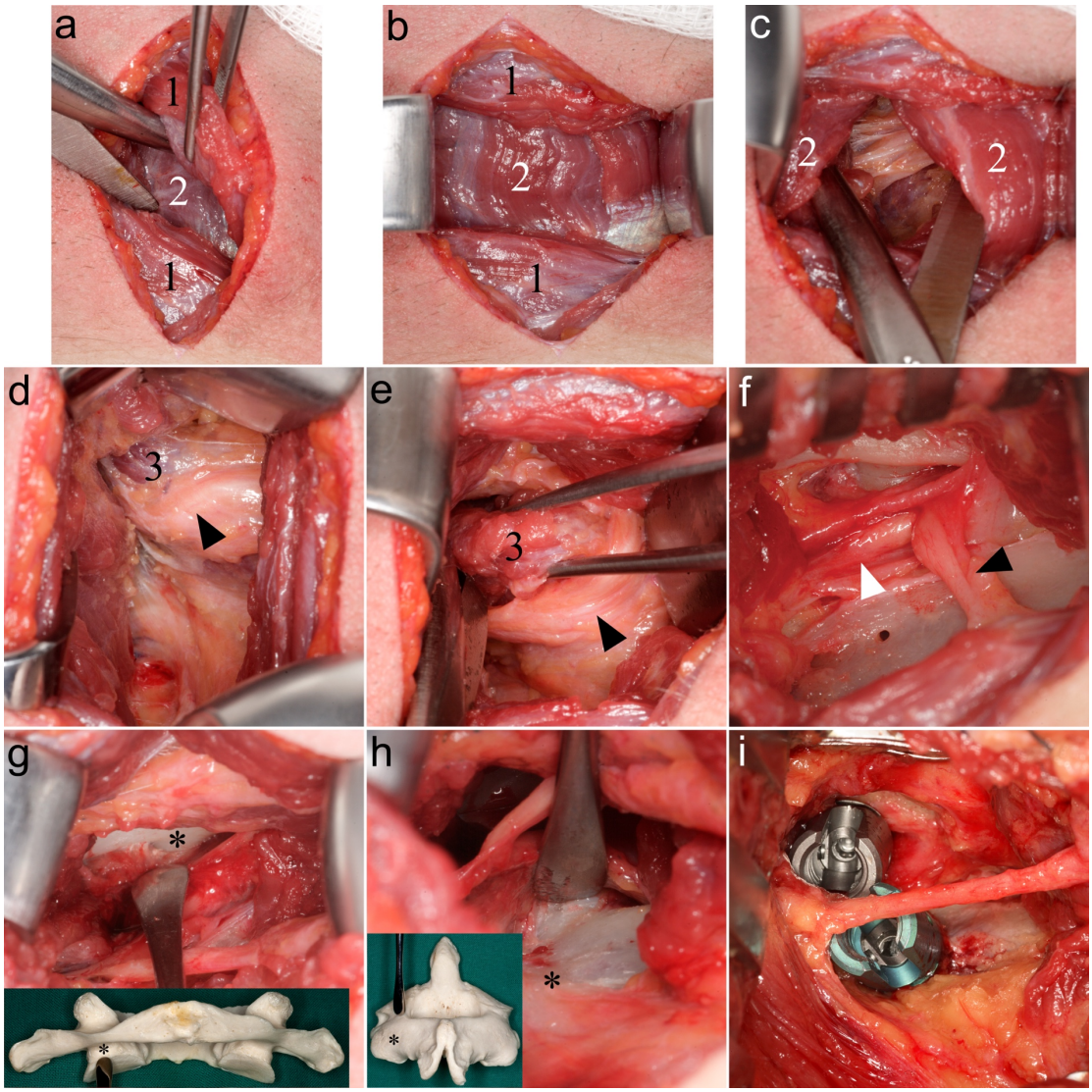

Figure 7. Steps of the operation demonstrated on a cadaver (left side). Orientation: Cranial direction is towards the upper margin of the images, while medial is on the right side. a - The skin is incised, and the splenius capitis muscle (1) is split with scissors. Deep to it, the fibers of the semispinalis capitis muscle (2) are visible; b - The splenius

capitis muscle is retracted, exposing the deeper structures; c -The semispinalis capitis muscle is split with scissors, further revealing deeper layers;
d - The obliquus capitis inferior muscle is now visible, covered by its white fascia. The greater occipital nerve (black arrowhead) runs cranially and medially along the muscle. Below the muscle, the C2-C3 joint becomes visible; e - The obliquus capitis inferior muscle is prepared, and its muscle belly is resected. The greater occipital nerve is indicated by an arrowhead; f - The posterior arch of the atlas and the lamina of the axis are exposed in deeper layers. The ventral ramus (white arrowhead) and dorsal ramus (black arrowhead) of the C2 spinal nerve are also visible; g - A dissector points to the posterior surface of the lateral mass of the atlas. The entry point for the C1 lateral mass screw is marked with an asterisk. An inset shows the same setup on bone; h - The dissector elevates the soft tissues from the pars interarticularis and lamina of the axis. The entry point for the C2 pars screw is marked with an asterisk. An inset displays the same setup on bone; i - The C1 lateral mass and C2 pars interarticularis screws are placed. The greater occipital nerve is preserved, running medially in the center of the image. Reprinted with permission; Bodon 2014 [60]

The next step was to determine whether the applicable anatomy of the C1-C2 complex, particularly the spatial correlations of important landmarks and the viability of a muscle-splitting strategy, made consistent and accurate screw placement possible. All crucial bony landmarks needed for C1-C2 fusion were easily recognized in each cadaver. The lateral mass of C1, the lamina of C2, the posterior arch of the atlas and the medial border of the pars interarticularis of C2 were among them.

The entrance points for the C1 lateral mass screws and the C2 pars interarticularis screws were successfully found in every specimen using the previously mentioned muscle-splitting procedure. Four cadavers were fitted with 3.5-mm micro polyaxial screws using the method described by Harms and Melcher [8]. Intraoperative C-arm fluoroscopy was used to validate the screw placement precision (Figure 8), indicating that this minimally invasive technique minimizes soft tissue damage while offering dependable access to the C1-C2 complex.

Figure 8. Intraoperative fluoroscopic imaging following the insertion of C1 lateral mass and C2 pars interarticularis screws. Reprinted with permission; Bodon 2014 [60]

4.2 Far lateral suboccipital approach

The posterolateral extradural suboccipital approach is a valuable technique for accessing the anterior epidural space and the retro-odontoid region, which are often challenging to reach through conventional methods. While this approach has been utilized in various surgical interventions, the extent of necessary bone removal from the atlas (C1) remains undefined. Given the intricate anatomy of the craniovertebral junction, precise adjustments in bone resection are crucial for optimizing surgical exposure while preserving structural stability.

To address this gap, the author of this thesis contributed to a cadaveric study evaluating the changes in the size of the horizontal and vertical surgical windows following stepwise bone removal of C1. The study aimed to determine the minimum necessary resection to achieve adequate visualization while maintaining bony integrity. Additionally, a representative clinical case was included to illustrate the practical application of these findings.

Below, the technical description of the far lateral suboccipital approach is presented, based on the author's previously published work [21].

A macerated bone specimen of the craniocervical junction was used for the anatomical and descriptive portion of the study. Additionally, five Thiel-fixed human cadaveric specimens were utilized for the anatomical and experimental investigation. These specimens ranged in age from 74 to 94 years, with an average age of 83.7 years. Measurements were taken on both sides of the body. Prior to dissection, the vertebral arteries (VA) were filled with colored silicone to enhance visualization.

The cadavers were positioned prone for the dissections, with the cervical spine in a neutral position. The head was stabilized using a modified Halo-fixation device. To allow for medial angulation of the working channel, sufficient soft tissue release was performed.

A posterior midline incision combined with a posterolateral suboccipital approach was used to access the posterior aspect of the craniocervical junction. Subperiosteal dissection was carried out on the occiput, posterior arch of the atlas (C1), and lamina of the axis (C2). Additionally, the V3v and V3h segments of the vertebral artery were carefully prepared for further anatomical assessment.

At the level of the C2 isthmus, the C2 nerve root was identified, running lateral to its ganglion. In all specimens, this nerve root was transected and used to gently retract the dural sac medially, allowing access to the epidural region (Figure 9a).

At this stage, with C1 intact, the epidural access window was medially bounded by the dural sac, laterally by the lateral atlanto-axial joint, cranially by the C1 posterior arch, and inferiorly by the lamina of C2 (Figure 9a). After measuring the horizontal and vertical dimensions of the surgical window, incremental bone removal of C1 was performed to expand the access. The surgical window was then remeasured to assess the changes in available space.

First, a 5 mm diamond burr (sphere formed, diamond coated drill bit) was used to create a semicircular laminotomy at the inferior aspect of the posterolateral section of the ipsilateral C1 posterior arch (Figure 9b). The laminotomy measured 10 mm in width and

3–4 mm in height, depending on the local anatomy. Second, a 2 mm Kerrison rongeur (used to take away bone from not easily accessible locations) and a high-speed burr (a surgical drill designed to remove bone using special drill tips) were used to remove the ipsilateral C1 posterior hemiarch (Figure 9c). At this stage, the V3h segment of the vertebral artery formed the cranial boundary of the surgical window, while the horizontal dimensions remained unchanged. Third, a high-speed burr was used to remove 3 mm of bone from the medial aspect of the C1 lateral mass (Figure 9d). This step expanded the horizontal surgical window, while the vertical dimensions remained unchanged. These three steps were first performed on the right side of the cadaver, followed by the left side.

Both the height of the odontoid process (from tip to base) and its thickness at the base were measured. Additionally, after opening the dura, the maximum thickness of the spinal cord in the coronal plane at the C1-C2 level was recorded.

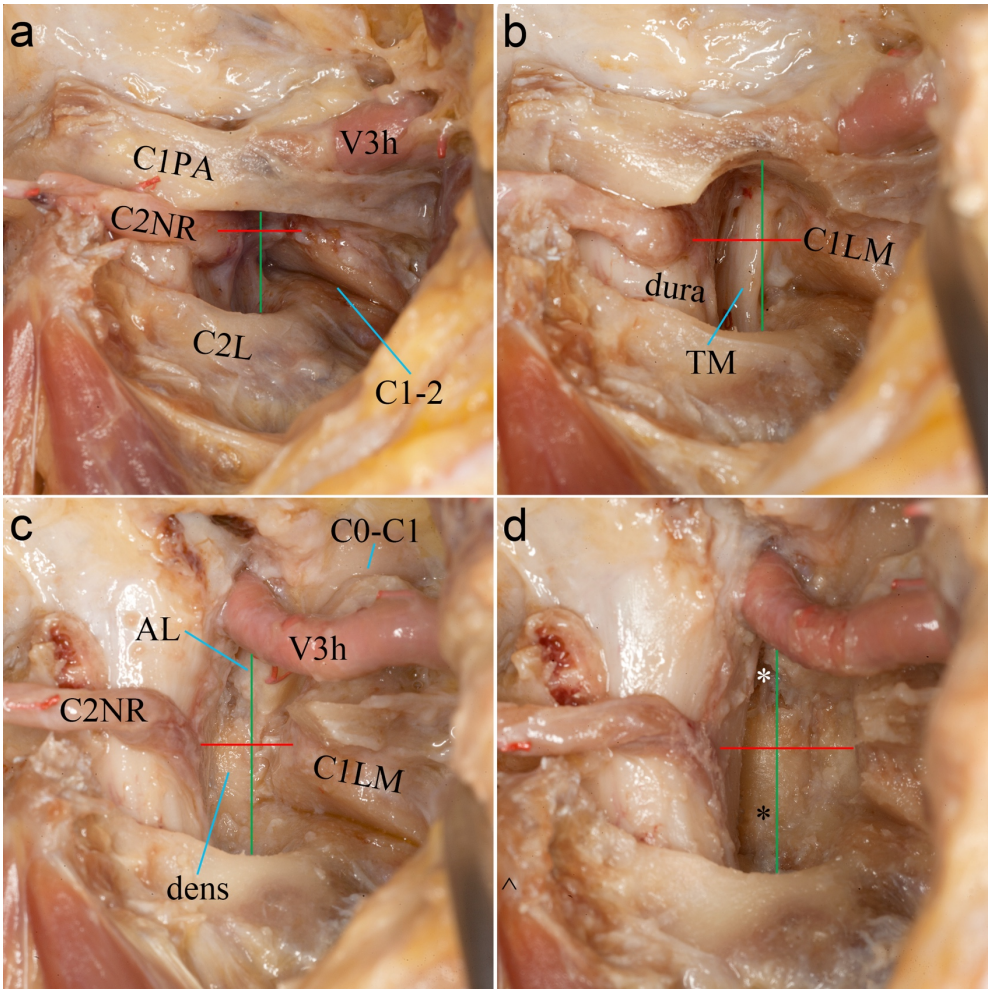

Figure 9. Steps of bone removal, right side. Red line marks the horizontal, green line the vertical window. C1PA refers to the C1 posterior arch, C2L to the C2 lamina, and C1LM to the C1 lateral mass. Ligaments and neural structures include the AL (alar ligament), C2NR (C2 nerve root), and TM (tectorial membrane). The V3h represents the horizontal segment of the vertebral artery. The visible joints include the C0–C1 atlantooccipital joint and the C1–C2 atlantoaxial joint. The white asterisk marks the tip of the dens, while the black asterisk indicates its base. Reprinted with permission; Bodon 2020 [21]

After establishing the surgical technique and measurements, the next step was to analyze the anatomical findings and clinical implications of the procedure. This included an assessment of the relevant bony and neural anatomy of C1-C2, followed by an evaluation of sequential C1 bone resection, classified into four types based on the extent of resection.

Significant bone differences were seen in the atlantoaxial area, especially in the distance between the C1 posterior arch and the C2 lamina. This distance increased with upper cervical spine flexion and varied according to head position. From a lateral perspective, the axis vertebra exhibited a gradual upward slope, with the superior border of the C2 lamina, the uppermost part of the pars interarticularis, and the base of the odontoid positioned at increasingly higher levels. Among these, the base of the odontoid was the most cranially located. This anatomical inclination means that a horizontal surgical trajectory just above the C2 lamina would lead to the upper portion of the C2 vertebral body, while the base of the odontoid remains positioned higher and obscured beneath the posterior arch of the atlas. Based on measurements, the odontoid's height was 14.4 ± 1.0 mm and its base thickness was 10.8 ± 1.4 mm. At the C1-C2 level, the spinal cord's maximal thickness was measured at 10.7 ± 0.3 mm [21].

The sequential process of C1 bone resection was classified into four distinct types based on the extent of bone removal. Type 1 involved no bone removal, serving as the baseline reference. Type 2 consisted of a semicircular inferior partial resection of the C1 posterior arch. Type 3 entailed the ipsilateral removal of the C1 posterior arch, allowing for greater surgical exposure. Finally, Type 4 involved a partial resection of the C1 lateral mass, further expanding the surgical window while maintaining structural integrity.

As the starting point of the classification, Type 1 represents the intact anatomical configuration without any bone resection. In this state, the surgical window was naturally restricted, limiting direct access to deeper structures.
Medially, the window was bounded by the dura, while laterally, it was confined by the C1-C2 joint. The cranial boundary was formed by the posterior arch of the atlas, whereas the caudal limit was defined by the C2 lamina.
Without any bone removal, the surgical exposure remained constrained, permitting only limited access to the anterior epidural space, reaching up to the base of the odontoid. The measured dimensions of the surgical window were 6.3 ± 2.1 mm horizontally and 9.7 ± 1.5 mm vertically.

Continuing from the intact configuration of Type 1, Type 2 involved a semicircular inferior partial resection of the C1 posterior arch, which was centered above the surgical window. This resection measured 10 mm in width and 3–4 mm in height.

The horizontal dimensions of the surgical window remained unchanged, with medial and lateral boundaries still defined by the dura and the C1-C2 joint, respectively. However, in the vertical plane, the cranial boundary was now formed by the C1 laminotomy defect, while the caudal limit remained the C2 lamina.

This laminotomy improved vertical access, allowing for better exposure of the anterior epidural space up to the base of the odontoid. The final surgical window dimensions measured 6.3 ± 2.1 mm horizontally and 13.0 ± 1.2 mm vertically.

Following the partial resection in Type 2, Type 3 involved the removal of the ipsilateral C1 posterior arch, extending from the posterior tubercle to its lateral base. This modification significantly increased the vertical dimensions of the surgical window, while the horizontal width remained unchanged.

In this configuration, the caudal boundary of the surgical window remained the C2 lamina, while the cranial limit was now defined by the V3h segment of the vertebral artery.

This expanded vertical access allowed direct visualization of the entire odontoid, reaching up to its tip. The final surgical window dimensions measured 6.3 ± 2.1 mm horizontally and 17.3 ± 1.1 mm vertically.

Type 4 involved bone removal from the medial aspect of the C1 lateral mass, resulting in a wider horizontal surgical window, while the vertical dimensions remained unchanged. The extent of horizontal widening was directly proportional to the amount of C1 bone removed. Approximately 3 mm of bone was drilled from the medial aspect of the C1 lateral mass.

Following this modification, the medial boundary of the surgical window remained the dura, while the lateral limit was now defined by the C1-C2 joint and a thinned C1 lateral mass.

This final step maximized access to the anterior epidural space, allowing full visualization of the odontoid from its base to its tip and its ipsilateral side. Additionally, the medial

aspect of the lateral mass and the distance between the odontoid and the lateral mass could now be accessed.

The final surgical window dimensions measured 10.3 ± 0.5 mm horizontally and 17.3 ± 1.1 mm vertically.

5. Discussion

Even after extensive research and advancements in spine surgery, the optimal approach for accessing the retro-odontoid region and achieving C1–C2 fusion remains a subject of ongoing discussion. Since the introduction of posterior C1–C2 fusion techniques, such as those described by Magerl [6] and later modified by Harms and Melcher [8], surgeons have continuously refined their methods to improve stability, minimize soft tissue damage, and enhance surgical precision. Likewise, the far lateral suboccipital approach has evolved as a means to safely access the anterior epidural space and retro-odontoid region, yet the extent of necessary bone removal remains a crucial question in optimizing exposure while preserving anatomical integrity.

Every advancement in the understanding of upper cervical spine anatomy and surgical techniques directly contributes to improving patient outcomes. By optimizing surgical access, preserving critical structures, and improving stability, the studies that the present dissertation is based on provide valuable knowledge that can lead to safer and more effective treatments, ultimately benefiting patients who require C1–C2 fusion or retro-odontoid decompression.

When it comes to improvement in surgical techniques, the first question that arises is how to minimize approach-related morbidity, especially in cases of intricate surgeries. Such approach-related injuries can come in the form of muscle-damage, destabilization of ligamentous structures, over-retraction, nerve- and vascular damage, excessive blood loss, postoperative pain and longer hospital stay. Minimally invasive approaches have been shown to decrease the prevalence and strength of these morbidities [11, 15-17]. The minimally invasive approaches for the most common posterior cervical procedures have been previously described by different authors [14, 17, 62, 63].

In C1-C2 fusion, the minimally invasive approach may possibly prevent postoperative loss of lordosis, as the multifidus and semispinalis cervicis muscles, as well as the posterior tension band and deep extensor muscles connected to the C2 spinous process are left intact [9, 64]. Another benefit of this surgery type is the reduction in muscle

retraction as the muscle layers and skin are opened directly above the entry points of the screws.

The author of the present paper identified two minimally invasive open (non-percutaneous) approaches for C1–C2 fusion which used the Harms technique. Both of these aim to reduce soft tissue disruption while maintaining surgical efficacy.

The first method used a typical midline skin incision and entered the surgical site through the intermuscular plane between the suboccipital neck muscles (obliquus capitis inferior) and the semispinalis cervicis. The C1–C2 and C2–C3 joints, the pars interarticularis, and the C2 lamina were all exposed as a result [14]. According to Shiraishi (2012), they conducted six C1–C2 fusions in their study, with an average operating time of 180 minutes and an average blood loss of 45 g [14].

Taghva [13], the Frempong-Boadu group [11, 12] created the second strategy, which is comparable to the one used in this investigation. The benefits of this approach have already been reported [11, 12, 14].

In case of the Frempong-Boadu group, the strategy includes two paramedian skin incisions, each 2.5 cm or 2 cm long and positioned 2 cm from the midline, were used in their procedure. The surgeons performed subperiosteal dissection to reveal the C2 and C3 lateral masses after first opening the fascia and then inserting increasingly larger dilators to reach the C2 lamina. In order to reach the inferior part of the C1 lateral mass, this technique also required sacrificing the C2 nerve root [11, 12].

As mentioned above, Taghva's method [13] resembles the previous method but contains slight modifications: it starts with a 3-cm-long skin incision that is 3.5cm from the midline, then the standard muscle-splitting dissection and sequential dilation follows to place a tubular retractor on the C2 lateral mass. This is done under fluoroscopic guidance. Both of these approaches use a fluoroscopy-guided tubular retractor method.

Similar to the minimally invasive approaches described by Shiraishi, Joseffer, Holly, and Taghva, the muscle-splitting technique described by the writer of this thesis aims to minimize soft tissue disruption while ensuring safe screw placement for C1–C2 fusion [11-14]. However, rather than relying on paramedian incisions and sequential dilation, this method follows a layered muscle-splitting approach, providing a direct and controlled exposure of key anatomical structures [60].

In this technique, each muscle layer is systematically identified, split, and retracted until the suboccipital muscles are reached. The obliquus capitis inferior muscle, a crucial landmark, is then either retracted or resected, depending on the surgical objective—temporary fixation or full fusion (Figure 10). This step allows for clear visualization of essential bony landmarks, including the posterior aspect of the atlas lateral mass, the C2–C3 joint, the C2 lamina, and the pars interarticularis of the axis [60].

By preserving the posterior musculature as much as possible, this technique ensures adequate surgical exposure while reducing soft tissue trauma. Using this approach, posterior C1–C2 fusion or fixation can be performed following the Harms and Melcher technique [8], combining structural integrity with improved postoperative recovery [60].

As with any procedure involving the upper cervical spine, precision and awareness of regional anatomy are crucial to avoiding complications. When positioning the retractor or manipulating the obliquus capitis inferior muscle, it is essential to avoid docking above the posterior arch of the atlas, as the vertebral artery frequently extends over this area and is at risk of injury [12].

A comprehensive understanding of the musculature and anatomical landmarks in the posterior upper cervical spine is key to safely performing this technique. Given the complex and variable anatomy of this region, blind muscle dilatation and expandable retractor placement under fluoroscopic guidance pose significant risks. Careful identification of key structures and precise surgical technique are critical to minimizing complications and ensuring safe and effective surgical access.

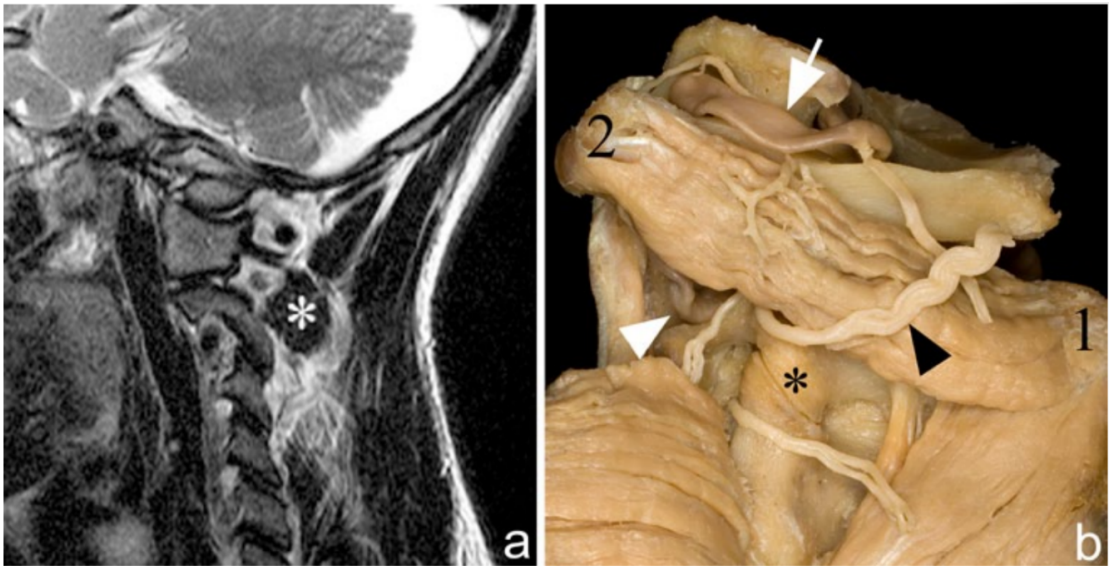

Figure 10. Anatomical and MRI visualization of the obliquus capitis inferior muscle. (a) Sagittal cervical MRI showing the obliquus capitis inferior muscle (white asterisk) at the level of the C1 lateral mass and C2 pars interarticularis, highlighting its relation to the posterior arch of the atlas and lamina of the axis. (b) Formalin-fixed specimen displaying the obliquus capitis inferior muscle between the spinous process of the axis (1) and the transverse process of the atlas (2). The posterior arch of the atlas is visible cranially. The V3 vertebral artery segments are marked: white arrow (horizontal part) and white arrowhead (vertical part). The black asterisk denotes the inferior articular process of the axis, while the black arrowhead points to the greater occipital nerve. Reprinted with permission; Bodon 2014 [60]

Building on the C1–C2 fusion study [60], which introduced a minimally invasive muscle-splitting technique to reduce approach-related morbidity while ensuring safe screw placement, the Far-Lateral Study [21] expands this understanding by systematically evaluating the impact of different degrees of C1 bony resection on surgical window dimensions. While the C1–C2 fusion study focused on preserving soft tissue integrity and optimizing screw trajectories, the Far-Lateral Study provides critical insight into how progressive bone removal can enhance access to the retro-odontoid region using a far lateral approach through a midline posterior incision.

The findings have significant clinical relevance, particularly for the planning and execution of complex procedures. By defining a structured stepwise resection strategy,

this research contributed to improving surgical precision and exposure, ensuring safer and more effective correction of complex cervical deformities.

One of the largest reported series on the transoccipitocervical posterolateral approach for anterior C0–C2 lesions involved 23 patients and described the efficacy of posterior decompression with craniocervical fusion [65]. The bony decompression in these cases included foramen magnum expansion, resection of the posterior arch of C1, removal of the posterior portion of the C1 lateral mass, and resection of the posterior aspect of the odontoid and posterosuperior part of the C2 vertebral body. This extensive posterior decompression allowed for anteroposterior relief of the medulla and spinal cord, ensuring adequate space for neural decompression, followed by stabilization through craniocervical fusion.

In the years following the initial transoccipitocervical posterolateral approach, several modifications were introduced to improve access and decompression for retro-odontoid pathologies. One such adaptation involved the removal of a retro-odontoid pseudotumor via a transdural approach, following complete resection of the C1 posterior arch while preserving the arachnoid [18].

Later, Archavlis [66] reported a posterior odontoidectomy using a tubular retractor system, performing bone resection of the C1–2 lateral masses and the C2 pars interarticularis in four cadaveric specimens, with subsequent clinical application in two patients.

A similar tubular retractor-based technique was later employed by Riley to treat a high cervical epidural abscess [20]. In this case, the medial aspect of the C1–2 joint and the inferior laminar edge of C1 were resected by 2–3 mm using a high speed burr, while 3 mm of the C1 lateral mass was removed through a 14-mm tubular retractor system to access the C1–2 epidural space and the odontoid. To improve surgical exposure, the upper cervical spine was flexed, and the head was tilted and rotated contralaterally, increasing the C1–2 interlaminar space.

Building on previous modifications of the transoccipitocervical approach, an anatomic feasibility study [21] was conducted with the head in a neutral position to allow for standardized measurements and accurate assessment of surgical window dimensions. While head positioning adjustments—such as flexion, contralateral tilt, and rotation—have been used in clinical cases to enhance C1–C2 interlaminar space and surgical access,

the author of the paper believes that such maneuvers could potentially introduce additional challenges in terms of vertebral artery and neural structure protection.

Rotation of the atlantoaxial joint alters the spatial relationships between the vertebral artery and adjacent bony landmarks, may make intraoperative navigation more complex and increasing the risk of vascular injury. Additionally, in patients with rigid craniocervical deformities, such as in the case of the far-lateral approach feasibility study, positional adjustments of C1 relative to C2 are ineffective, further emphasizing the need for precise surgical planning and individualized bone resection strategies [21].

Similarly, to the knowledge of the author, the study was the first to describe an odontoid and anterior C1–2 column osteotomy using a posterolateral suboccipital approach with a midline incision. Here, a transoral approach and anterior release of the C1–2 structures were not feasible due to the severe flexion deformity and the patient's rigid chin-on-chest positioning, which limited anterior access. Furthermore, a posterolateral approach was preferred over the transoral route due to its better control of the dural sac and a lower risk of infection [21].

Expanding on the stepwise classification of C1 bone resection, the findings further refine the surgical decision-making process by identifying three distinct forms of bone removal, each tailored to specific surgical objectives. Depending on the extent of exposure needed, different levels of C1 resection can optimize surgical access while preserving structural integrity.

In order to expose the odontoid base and provide access to the anterior epidural space, the semicircular inferior partial excision of the C1 arch should be modified in accordance with anatomical differences of the C1 posterior arch. Notably, vascular protection during operations anterior to the dural sac and inside the retro-odontoid region is improved by maintaining a bone margin cranially beneath the vertebral artery [21].

Unilateral C1 posterior arch removal is essential to increase the vertical surgical window and provide access to the odontoid tip if total odontoid resection is needed. Nonetheless, the horizontal section of the vertebral artery (V3v) continues to limit this vertical window cranially. When odontoid removal is the surgical objective, resecting the medial portion of the C1 lateral mass can expand the horizontal window and further increase exposure. An expanded surgical window is necessary for safe and effective excision because the odontoid's mean maximal width in the coronal and sagittal planes is 11 mm [35].

The author's findings show that the initial horizontal window with intact bone structures is just 6 mm and the mean odontoid height is 14.4 ± 1.0 mm. But when the medial C1 lateral bulk is removed, this gap widens to 10 mm, greatly enhancing access. Without these modifications, it could be difficult or impossible to conduct odontoid excision using a far lateral approach and posterior midline incision [21].

Accessing the odontoid process and dissecting its surrounding soft tissues inevitably compromises the primary stabilizers of the upper cervical spine, including the tectorial membrane, craniocervical Y-ligament [29], transverse ligament, and alar ligaments. Disruption of these ligamentous structures can result in craniovertebral and atlantoaxial instability, often necessitating C0–C2 or C1–C2 fusion to restore stability and prevent post-surgical instability. Importantly, if fusion is required, it can be seamlessly performed using the same posterior approach, eliminating the need for an additional surgical corridor [21].

Both studies emphasized the importance of preserving critical neurovascular structures during upper cervical spine surgery. In the minimally invasive C1–C2 fusion study, the muscle-splitting approach allowed for safe screw placement, confirmed via intraoperative fluoroscopy, without causing iatrogenic fractures or vascular injury [60].

Both studies relied on cadaveric specimens to evaluate anatomical feasibility and surgical exposure. While this method allows for precise anatomical measurements, it does not fully replicate live surgical conditions, where factors such as tissue elasticity, bleeding, and intraoperative swelling can influence surgical accessibility and instrumentation. Furthermore, the absence of postoperative healing and fusion dynamics in cadaveric studies limits the ability to assess long-term biomechanical stability [21, 60].

Another limitation is that the C1–C2 complex exhibits significant anatomical variability, particularly in the thickness of the posterior arch, the size of the lateral mass, and the course of the vertebral artery [21]. While this study classified stepwise C1 bone resection to optimize surgical exposure, the applicability of these findings to a broader patient population remains uncertain. In some cases, additional bony anomalies or congenital variations may require modifications to the standard resection strategy. Similarly, the

feasibility of the muscle-splitting technique may vary in patients with fibrotic or hypertrophic musculature [21].

Both the far lateral suboccipital approach and the muscle-splitting technique require specific anatomical knowledge and technical skill, which may limit widespread adoption among spine surgeons [21, 60]. The risk of vertebral artery injury, dura violation or neural damage remains a concern, particularly in cases with severe anatomical variations. Further training and refinement of these techniques, possibly with navigation-assisted surgery may help improve surgical precision and safety.

The findings of these studies highlight important advancements in upper cervical spine surgery, particularly in minimally invasive C1–C2 fusion techniques and far lateral suboccipital approaches to the retro-odontoid region. However, further research is needed to validate these approaches in clinical settings, optimize surgical precision, and explore technological innovations that can enhance safety and outcomes.

While the cadaveric studies provided detailed anatomical insights, the next step is to conduct prospective clinical studies to assess the efficacy, safety, and long-term impact of these techniques in real-world surgical practice. This includes evaluating fusion rates, biomechanical stability, and complication risks in patients undergoing C1–C2 fusion with the muscle-splitting approach [60] and assessing functional recovery, pain relief, and neurological outcomes in cases where the far lateral suboccipital approach is used for retro-odontoid decompression [21].

Precision is crucial in C1–C2 surgery due to its complex bony and vascular anatomy. Future research should explore technology-assisted techniques such as three-dimensional navigation for intraoperative guidance, augmented reality and robotic-assisted surgery for improved trajectory planning, and preoperative 3D modeling for patient-specific implants, especially in cases with severe deformities.

The stepwise classification of C1 bone resection provides a structured method for expanding the surgical window, but further research should assess its biomechanical

impact, refine partial vs. complete C1 lateral mass preservation and analyze how anatomical variations influence bone removal strategies.

The muscle-splitting approach has shown promise in preserving soft tissue integrity, yet additional studies should compare postoperative recovery between muscle-splitting and midline techniques, evaluate its applicability in subaxial cervical fusion and occipito-cervical stabilization, and determine if muscle preservation enhances long-term cervical mobility.

6. Conclusions

This thesis explored two key surgical advancements in upper cervical spine surgery: the far lateral suboccipital approach to the retro-odontoid region and a muscle-splitting approach for C1–C2 fusion. Both studies provided anatomical validation and technical feasibility for improving surgical access, preserving soft tissue integrity and optimizing instrumentation in a region known for its complex anatomy and high surgical risk.
The stepwise classification of C1 bone resection established in the far lateral suboccipital approach study offers a structured method for tailoring surgical exposure while maintaining stability. The findings demonstrate that progressive removal of the C1 posterior arch and lateral mass can significantly enhance surgical access to the retro-odontoid region, reducing the need for high-risk anterior approaches.

The muscle-splitting approach for C1–C2 fusion was shown to be a viable alternative to traditional midline exposure, providing safe and effective screw placement while reducing muscle trauma. The intraoperative findings confirmed that this approach preserves posterior musculature, which may contribute to less postoperative pain and faster recovery compared to conventional methods.

While the studies provided important anatomical and surgical insights, clinical validation through long-term patient follow-up is necessary to confirm their safety, efficacy, and biomechanical stability. Additionally, integrating navigation-assisted surgery and 3D modeling could further enhance precision and reduce intraoperative risks.

In conclusion, the findings of this thesis support the adoption of minimally invasive approaches for C1–C2 surgery, offering new strategies for reducing morbidity, optimizing exposure, and improving patient outcomes. These advancements have the potential to refine surgical standards and contribute to the future evolution of upper cervical spine procedures.

7. Summary

The upper cervical spine presents unique surgical challenges due to its complex anatomy, biomechanical significance, and proximity to critical neurovascular structures. This thesis investigates two key advancements aimed at improving surgical access and stabilization in the C1–C2 region: the far lateral suboccipital approach to the retro-odontoid region and the muscle-splitting technique for C1–C2 fusion. Through cadaveric dissections and clinical applications, this research provides anatomical validation, technical feasibility, and potential clinical benefits of these approaches.

The first study examined the feasibility of a minimally invasive, muscle-splitting approach for C1–C2 fusion. This technique aims to reduce muscle trauma by splitting rather than detaching key posterior cervical muscles, potentially leading to less postoperative pain, faster recovery, and preserved cervical function. The study confirmed that this approach provides adequate access for safe screw placement, with intraoperative fluoroscopy verifying accurate instrumentation [60].

The second study focused on optimizing the far lateral suboccipital approach, addressing the lack of a standardized method for bone removal to improve access to the retro-odontoid region. By classifying stepwise C1 bone resection (Types 1–4), this study established a structured framework for expanding the surgical window while preserving stability. The findings suggest that progressive resection of the C1 posterior arch and lateral mass significantly increases surgical exposure, offering a safer alternative to transoral decompression [21].

The findings of this thesis contribute to advancing surgical strategies for the upper cervical spine, offering new methods for improving surgical access, reducing morbidity, and optimizing patient outcomes. These approaches have the potential to refine current surgical standards and shape the future of minimally invasive spine surgery.

8. References

1. Mixter SJ, Osgood RB. Traumatic lesions of the atlas and axis. Ann. Surg. 1910;51(2):193–207.
2. Gallie WE. Fractures and dislocations of the cervical spine. Am. J. Surg. 1939;46:495–499.
3. Brooks AL, Jenkins EB. Atlanto-axial arthrodesis by the wedge compression method. J. Bone Jt. Surg. 1978; 60(3):279–284.
4. Coyne TJ, Fehlings MG, Wallace MC, Bernstein M, Tator CH. C1-C2 posterior cervical fusion: long-term evaluation of results and efficacy. Neurosurgery. 1995;37(4):688–692 (Discussion 692–693).
5. Melcher RP, Puttlitz CM, Kleinstueck FS, Lotz JC, Harms J, Bradford DS. Biomechanical testing of posterior atlanto-axial fixation techniques. Spine. 2002;27:2435–2440.
6. Magerl F, Seeman PS. Stable posterior fusion of the atlas and axis by transarticular screw fixation. In: Kehr P, Weidner A, editors. Cervical Spine I. Heidelberg: Springer; 1987. p. 322–327.
7. Goel A, Laheri V. Plate and screw fixation for atlanto-axial subluxation. Acta Neurochir (Wien). 1994;129(1–2):47–53.
8. Harms J, Melcher RP. Posterior C1-C2 fusion with pol-yaxial screw and rod fixation. Spine. 2001;26(22):2467–2471.
9. Takeshita K, Peterson ETK, Bylski-Austrow D, Crawford AH, Nakamura K. The nuchal ligament restrains cervical spine flexion. Spine. 2004;29(18):E388–E393.
10. O'Toole J, Voyadzis JM, Gala VC. Posterior minimally invasive cervical foraminotomy and laminectomy. In: Sandhu FA, Voyadzis JM, Fessler RG, editors. Decision Making for Minimally Invasive Spine Surgery. New York: Thieme; 2011.
11. Joseffer SS, Post N, Cooper PR, Frempong-Boadu AK. Minimally invasive atlantoaxial fixation with a polyaxial screw-rod construct: technical case report. Neurosurgery. 2006;58(4 Suppl 2).
12. Holly LT, Isaacs RE, Frempong-Boadu AK. Minimally invasive atlantoaxial fusion. Neurosurgery. 2010;66(3 Suppl):193–197.

13. Taghva A, Attenello FJ, Zada G, Khalessi AA, Hsieh PC. Minimally invasive posterior atlantoaxial fusion: a cadaveric and clinical feasibility study. World Neurosurg. 2013;80(3-4):414–421.
14. Shiraishi T, Kato M, Yato Y, Ueda S, Aoyama R, Yamane J, Kitamura K. New techniques for exposure of posterior cervical spine through intermuscular planes and their surgical application. Spine. 2012;37(5):E286–E296
15. Gejo R, Kawaguchi Y, Kondoh T, Tabuchi E, Matsui H, Torii K, Ono T, Kimura T. Magnetic resonance imaging and histologic evidence of postoperative back muscle injury in rats. Spine. 2000;25(8):941–946
16. Guiot BH, Khoo LT, Fessler RG. A minimally invasive technique for decompression of the lumbar spine. Spine. 2002;27(4):432–438
17. Shiraishi T, Fukuda K, Yato Y, Nakamura M, Ikegami T. Results of skip laminectomy-minimum 2-year follow-up study compared with open-door laminoplasty. Spine. 2003; 28(24):2667–2672
18. Fujiwara Y, Manabe H, Sumida T, Tanaka N, Hamasaki T. Microscopic Posterior Transdural Resection of Cervical Retro-Odontoid Pseudotumors. J Spinal Disord Tech. 2015;28(10):363–369.
19. Archavlis E, Serrano L, Schwandt E, Nimer A, Molina-Fuentes MF, Rahim T, Ackermann M, Gutenberg A, Kantelhardt SR, Giese A. A novel minimally invasive, dorsolateral, tubular partial odontoidectomy and autologous bone augmentation to treat dens pseudarthrosis: cadaveric, 3D virtual simulation study and technical report. J Neurosurg Spine. 2017;26(2):190–198.
20. Riley K, Singh H, Meyer SA, Jenkins AL 3rd. Minimally Invasive Surgical Approach for Odontoid Lesions: A Technical Description in a Case of High Cervical Osteomyelitis and Abscess. World Neurosurg. 2016;91:332–339.
21. Bodon G, Kiraly K, Ruttkay T, Hirt B, Koller H. Feasibility of the Far Lateral Suboccipital Approach to the Retroodontoid Region. How Much Bone Removal Is Truly Needed? Neurospine. 2020;17(4):921–928.
22. Cirpan S, Yonguc GN, Mas NG, Aksu F, Magden AO. Morphological and morphometric analysis of foramen magnum. J Craniofacial Surg. 2016;27(6):1576–1578.

23. Lega BC, Kramer DR, Newman JG, Lee JYK. Morphometric measurements of the anterior skull base for endoscopic transoral and transnasal approaches. Skull Base. 2011;21(1):65–70.
24. Zhou J, Orías AaE, Kang X, He J, Zhang Z, Inoue N, An HS. CT-based morphometric analysis of the occipital condyle: focus on occipital condyle screw insertion. J Neurosurg Spine. 2016;25(5):572–579.
25. Russo VM, Graziano F, Russo A, Albanese E, Ulm AJ. High anterior cervical approach to the clivus and foramen magnum: a microsurgical anatomy study. Oper Neurosurg. 2011;69:ons103–ons116.
26. Ellis H. Gray's Anatomy. 37th ed. Williams PL, Warwick R, Dyson M, Bannister LH, editors. Illustrated. Edinburgh: Churchill Livingstone; 1989. [Review in: Br J Surg. 1989;76(12):1359].
27. Tubbs RS, Salter EG, Oakes WJ. The accessory atlantoaxial ligament. Neurosurgery. (2004;55(2):400–404.
28. Morita T, Takebayashi T, Takashima H, Yoshimoto M, Ida K, Tanimoto K, Ohnishi H, Fujiwara H, Nagae M, Yamashita T. Mapping occipital bone thickness using computed tomography for safe screw placement. J Neurosurg Spine. 2015;23(2):254–258.
29. Bodon G, Hirt B. Surgical Anatomy of the Upper Cervical Spine and the Craniocervical Junction. In: Koller H, Robinson Y, editors. Cervical Spine Surgery: Standard and Advanced Techniques. Cham: Springer Nature Switzerland; 2019. p. 23-32.
30. Lin JM, Hipp JA, Reitman CA. C1 lateral mass screw placement via the posterior arch: a technique comparison and anatomic analysis. Spine J. 2013;13(11):1549–1555.
31. Yamaguchi S, Eguchi K, Kiura Y, Takeda M & Kurisu K. Posterolateral protrusion of the vertebral artery over the posterior arch of the atlas: quantitative anatomical study using three-dimensional computed tomography angiography. J Neurosurg Spine. 2008;9(2):167–174
32. Bodon G, Grimm A, Hirt B, Seifarth H, Barsa P. Applied anatomy of screw placement via the posterior arch of the atlas and anatomy-based refinements of

the technique. Eur J Orthop Surg Traumatol. 2016;26(7):793–803.

33. Le Minor JM. The retrotransverse foramen of the human atlas vertebra. A distinctive variant within primates. Acta Anat. 1997;160(3):208–212.
34. Arnautović KI, al-Mefty O, Pait TG, Krisht AF, Husain MM. The suboccipital cavernous sinus. Jo neurosurg. 1997;86(2):252–262.
35. Kandziora F, Schulze-Stahl N, Khodadadyan-Klostermann C, Schröder R, Mittlmeier T. Screw placement in transoral atlantoaxial plating systems: an anatomical study. J Neurosurg Spine. 2001;95(1):80–87.
36. Voth D, Glees P, von Goethe JW. Diseases in the Cranio-Cervical Junction. Berlin: Walter de Gruyter; 1987.
37. Seal C, Zarro C, Gelb D, Ludwig S. C1 lateral Mass anatomy. J Spinal Disord Tech. 2009;22(7):516–523.
38. Tan M, Wang H, Wang Y, Zhang G, Yi P, Li Z, Wei H, Yang F. Morphometric evaluation of screw fixation in atlas via posterior arch and lateral mass. Spine. 2003;28(9):888–895.
39. Ma XY, Yin QS, Wu ZH, Xia H, Liu JF, Xiang M, Zhao WD, Zhong SZ. C1 pedicle screws versus C1 lateral mass screws: comparisons of pullout strengths and biomechanical stabilities. Spine. 2009;34(4):371–377.
40. Lee MJ, Cassinelli E, Riew KD. The feasibility of inserting atlas lateral mass screws via the posterior arch. Spine. 2006;31(24):2798–2801.
41. Christensen DM, Eastlack RK, Lynch JJ, Yaszemski MJ, Currier BL. C1 anatomy and dimensions relative to lateral mass screw placement. Spine. 2007;32(8):844–848.
42. Ulbrich EJ, Schraner C, Boesch C, Hodler J, Busato A, Anderson SE, Eigenheer S, Zimmermann H, Sturzenegger M. Normative MR cervical spinal canal dimensions. Radiology. 2014; 271(1), 172–182.
43. Lang J. Clinical Anatomy of the Cervical Spine. George Thieme Verlag. (1993)
44. Heller JG, Alson MD, Schaffler MB, Garfin SR. Quantitative internal dens morphology. Spine. 1992;17(8):861–866.
45. Borne GM, Bedou GL, Pinaudeau M. Treatment of pedicular fractures of the axis. J Neurosurg. 1984;60(1):88–93.

46. Suchomel P, Choutka O. Reconstruction of upper cervical spine and craniovertebral junction. Berlin, Heidelberg: Springer; 2010.
47. Ebraheim NA, Whitehead JL, Alla SR, Moral MZ, Castillo S, McCollough AL, Yeasting RA, Liu J. The suprascapular nerve and its articular branch to the acromioclavicular joint: an anatomic study. J Shoulder Elbow Surg. 2011;20(2):e13-17.
48. Neo M, Matsushita M, Iwashita Y, Yasuda T, Sakamoto T, Nakamura T. Atlantoaxial transarticular screw fixation for a High-Riding Vertebral artery. Spine. 2003;28(7):666–670.
49. Moftakhar P, Gonzalez NR, Khoo LT, Holly, LT. Osseous and vascular anatomical variations within the C1–C2 complex: a radiographical study using computed tomography angiography. Int J Med Robot Comput Assist Surg. 2008;4(2):158–164.
50. Ould-Slimane M, Pape SL, Leroux J, Foulongne E, Damade C, Dujardin F, Duparc F. CT analysis of C2 pedicles morphology and considerations of useful parameters for screwing. Surg Radiol Anat. 2013;36(6):537-542.
51. Smith ZA, Bistazzoni S, Onibokun A, Chen N, Sassi M, Khoo LT. Anatomical considerations for subaxial (C2) pedicle screw placement. J Spinal Disord Tech. 2010;23(3):176–179.
52. Cassinelli EH, Lee M, Skalak A, Ahn NU, Wright NM. Anatomic considerations for the placement of C2 laminar screws. Spine. 2006;31(24):2767–2771.
53. Lang J. Skull Base and Related Structures. Stuttgart: Schattauer Verlag; 2001.
54. Cattrysse E, Barbero M, Kool P, Gagey O, Clarys J, Van Roy P. 3D morphometry of the transverse and alar ligaments in the occipito–atlanto–axial complex: An in vitro analysis. Clin Anat. 2007;20(8):892–898.
55. Tubbs RS, Hallock JD, Radcliff V, Naftel RP, Mortazavi M, Shoja MM, Loukas M, Cohen-Gadol AA. Ligaments of the craniocervical junction. 2011;14(6):697–709.
56. Fick R. Handbuch der Anatomie und Mechanik der Gelenke, unter Berücksichtigung der bewegenden Muskeln. 2024 ed. Vero Verlag GmbH & Co.KG; 2014. (Original work published 1904).

57. Arnold F. Handbuch der Anatomie des Menschen. Freiburg im Breisgau: Herdersche Verlagshandlung; 1851.
58. Yuksel M, Heiserman JE, Sonntag VK. Magnetic resonance imaging of the craniocervical junction at 3-T: observation of the accessory atlantoaxial ligaments. Neurosurgery. 2006;59(4):888–893.
59. Fisahn C, Schmidt C, Rostad S, Li R, Rustagi T, Alonso F, Mohammadali MS, Iwanaga J, Chapman JR, Oskouian RJ, Tubbs RS. The Adult Apical Ligament of the Dens Does Not Contain Notochordal Tissue: Application to Better Understanding the Origins of Skull Base Chordomas. World Neurosurg. 2017;101:42-46.
60. Bodon G, Patonay L, Baksa G, Olerud C. Applied anatomy of a minimally invasive muscle-splitting approach to posterior C1-C2 fusion: an anatomical feasibility study. Surg Radiol Anat. 2014;36(10):1063–1069.
61. Hammer N. Thirty years of Thiel embalming-A systematic review on its utility in medical research. Clin Anat. 2022;35(7):987-997.
62. Santiago P, Fessler RG. Minimally invasive surgery for the management of cervical spondylosis. Neurosurgery. 2007;60:S160–S165
63. Wang MY, Levi ADO. Minimally invasive lateral mass screw fixation in the cervical spine: initial clinical experience with long-term follow-up. Neurosurgery. 2006;58(5):907–912
64. Iizuka H, Shimizu T, Tateno K, Toda N, Edakuni H, Shimada H, Takagishi K. Extensor musculature of the cervical spine after laminoplasty: morphologic evaluation by coronal view of the magnetic resonance image. Spine. 2001;26(20):2220–2226.
65. Limin L, Chunguang Z, Yueming S, Siqing H, Hao L, Quan G, Tao L, Jiancheng Z, Faming L. A posterolateral approach to occipitoatlantoaxial ventral lesions. J Spinal Disord Tech. 2013;26(5):281–290.
66. Archavlis E, Nievas MC. Kranioplastik nach supratentorieller dekompressiver Kraniektomie. Nervenarzt. 2012;83(6):751-758.

9. Bibliography of the candidate´s publications

Publications related to this dissertation:

Bodon G, Patonay L, Baksa G, Olerud C. Applied anatomy of a minimally invasive muscle-splitting approach to posterior C1-C2 fusion: an anatomical feasibility study. Surg Radiol Anat. 2014;36(10):1063–1069.
Impact factor: 1,047

Bodon G, Hirt B. Surgical anatomy of the upper cervical spine and the craniocervical junction. In: Koller H, Robinson Y, editors. Cervical Spine Surgery: Standard and Advanced Techniques. Cham: Springer Nature Switzerland; 2019. p. 23–32.

Bodon G, Kiraly K, Ruttkay T, Hirt B, Koller H. Feasibility of the far lateral suboccipital approach to the retroodontoid region: how much bone removal is truly needed? Neurospine. 2020;17(4):921–928.
Impact factor: 3,492

Publications not related to this dissertation:

Bodon G, Glasz T, Olerud C. Anatomical changes in occipitalization: is there an increased risk during the standard posterior approach? Eur Spine J. 2013;22(Suppl 3):S512–S516.
Impact factor: 2,473

Bodon G, Degreif J, Seifarth H, Pitzen T. Is that only a spinous process fracture? Report of a case of a C6 spinous process fracture with accompanying complex ligamentous injury resulting in a delayed unilateral facet dislocation at the C6-7 level. Trauma Cases Rev. 2015;1:1014.
Impact factor: 0

Bodon G, Grimm A, Hirt B, Seifarth H, Barsa P. Applied anatomy of screw placement via the posterior arch of the atlas and anatomy-based refinements of the technique. Eur J Orthop Surg Traumatol. 2016;26(7):793–803.
Impact factor: 0

Bodon G, Choi PJ, Iwanaga J, Tubbs RS. The atlanto-occipital joint: a concise review of its anatomy and injury. Anatomy. 2017;11(3):141–145.
Impact factor: 0

Bodon G, Kiraly K, Tunyogi-Csapo M, Hirt B, Wilke H, Harms J, Patonay L. Introducing the craniocervical Y-ligament. Surg Radiol Anat. 2018;41(2):197–202.
Impact factor: 1,092

Koller H, Shiban E, **Bodon G**, Wostrack M, Krieg S, Meiners T, Meyer B. Neurovascular complications in complex spinal deformity surgery - prevention and treatment recommendations. Die Wirbelsäule. 2019;3(4):275–301.
Impact factor: 0

Bodon G, Kiraly K, Baksa G, Barany L, Kiss M, Hirt B, Pussert A, Timothy J, Stubbs L, Khajavi K, Braly B. Applied anatomy and surgical technique of the lateral single-position L5-S1 fusion. Clin Anat. 2021;34(5):774–784.
Impact factor: 2,409

MacDowall A, Barany L, **Bodon G**. Surgical treatment outcome on a national cohort of 176 patients with cervical manifestation of rheumatoid arthritis. J Craniovertebr Junction Spine. 2021;12(3):248–256.
Impact factor: 0

Bodon G, Degreif J. Fluoroscopy-based percutaneous posterior screw placement in the lateral position using the tunnel view technique: technical note. Eur Spine J. 2022;31(9):2204–2211.
Impact factor: 2,8

Kitamura K, de Dios E, **Bodon G**, Barany L, MacDowall A. Evaluating a paradigm shift from anterior decompression and fusion to muscle-preserving selective laminectomy: a single-center study of degenerative cervical myelopathy. J Neurosurg Spine. 2022;37(5):740–748.
Impact factor: 2,8

Guiroy A, Thomas JA, **Bodon G**, Patel A, Rogers M, Smith W, Seale J, Camino-Willhuber G, Menezes CM, Galgano M, Asghar J. Single-position transpsoas corpectomy and posterior instrumentation in the thoracolumbar spine for different clinical scenarios. Oper Neurosurg (Hagerstown). 2023;24(3):310–317.
Impact factor: 2,2

Book chapters:

Bodon G, Welk T, Seifarth H, Barsa P, Olerud C. Injuries to the craniocervical ligaments: radiological diagnosis and treatment. In: Tubbs RS, Iwanaga J, Loukas M, Oskouian R, editors. Clinical Anatomy of the Ligaments of the Craniocervical Junction. Newcastle upon Tyne: Cambridge Scholars Publishing; 2019. p. 284–302.

Bodon G, Combalia A. Relevant surgical anatomy of the posterior subaxial spine and the cervicothoracic junction. In: Koller H, Robinson Y, editors. Cervical Spine Surgery: Standard and Advanced Techniques. Cham: Springer Nature Switzerland; 2019. p. 43–49.

Bodon G, Combalia A. Relevant surgical anatomy of the anterior cervical spine, the high retropharyngeal and the subaxial regions. In: Koller H, Robinson Y, editors. Cervical Spine Surgery: Standard and Advanced Techniques. Cham: Springer Nature Switzerland; 2019. p. 33–41.

Bodon G, Hirt B. Surgical anatomy of the upper cervical spine and the craniocervical junction. In: Koller H, Robinson Y, editors. Cervical Spine Surgery: Standard and Advanced Techniques. Cham: Springer Nature Switzerland; 2019. p. 23–32. Bodon G, Jeszenszky D. Surgical approach: posterior far-lateral suboccipital approach. In: Koller H, Robinson Y, editors. Cervical Spine Surgery: Standard and Advanced Techniques. Cham: Springer Nature Switzerland; 2019. p. 89–96.

10. Acknowledgements

This thesis would not have been possible without the support, love and patience of my wife Dóra, my son Levente and my daughter Lilla. I hope I will be able to spend some more time with them after this is done.

Somehow, I wish I could thank my mother and my father for their support through the many years which allowed it for me to be where I am now. I´m sorry you two could not be here with me today.

I would like to thank all my colleagues, coauthors and senior authors. My greatest gratitude goes to Gábor Baksa, András Grimm, Tamás Király, Péter Kurucz, Dávid Lendvay, Péter Pálházy, Gyöngyvér Molnár, Örs Petneházy, Denis Berdajs and Róbert Reisch - from the Laboratory for Applied and Clinical Anatomy - for being my friends during my university years and well after. I would like to say thank you to Alán Alpár for giving me the right advice every second year and for Dezső Jeszenszky for starting me on „the right way". A special thank goes to Miklós Tóth who showed me how to sharpen a dissecting knife and how to make anatomic preparations. This PhD would not have been possible without my esteemed supervisor Tamás Ruttkay who was unbreakably supporting me in the last few years.

I would like to thank my first head of department from Klinikum Langensteinbach, Prof. Jürgen Harms. I hope I will be able to preserve a similar level of enthusiasm and never fading interest in spine surgery through the many decades of my professional life.

Lastly, I would love to thank Lajos Patonay, the head of the Laboratory for Applied and Clinical Anatomy for supporting me in the last more than 20 years, in good and in very bad times, throughout my university years and still. I have no idea where I would be without your help (and our regular calls mornings at 07:00 am). I am having a hard time to formulate words and sentences to tell you how much it means to me. Lalibáási, I´m proud and honored to call you my friend.